Research article

Application of green synthesized Ag and Cu nanoparticles for the control of bruchids and their impact on seed quality and yield in greengram

M. Hemalatha [a,*], J.S. Hilli [b], S.S. Chandrashekhar [a], A.G. Vijayakumar [c], Uday G. Reddy [d], P.S. Tippannavar [e]

[a] *Department of Seed Science and Technology, College of Agriculture, University of Agricultural Sciences (UAS), Dharwad, 580 005, Karnataka, India*
[b] *College of Agriculture, Hanumanamatti, UAS, Dharwad, 580 005, Karnataka, India*
[c] *Seed Unit, UAS, Dharwad, India*
[d] *AICRP Wheat, UAS, Dharwad, India*
[e] *Entomology and Sr. Farm Suptd., MARS, UAS, Dharwad, India*

ARTICLE INFO

ABSTRACT

Storage pests, particularly bruchids, are major biotic constraints causing significant storage losses in pulses. Conventional control methods relying on insecticides and fumigants often lead to food contamination due to toxic pesticide residues and a rapid decline in seed germination. In this investigation, through green nano-technological application, a promising and sustainable alternative for pest management is developed. Silver and copper nanoparticles were synthesized through ocimum leaf extract. The characterization of silver and copper nanoparticles was carried out by UV-spectroscopy, particle size analyzer, scanning electron microscopy, X-ray diffraction, and Fourier-transform infrared. Both the nanoparticles were spherical and crystalline in nature. Greengram seeds were primed with standardized silver and copper nanoparticles at different concentrations (1000, 1500, and 2000 ppm) and compared with castor-treated, deltamethrin-treated, and untreated control seeds for seed quality, growth, and yield. After one month of storage, all the pulse beetles released in different treatments exhibited 100 % mortality, whereas in control, the insects multiplied. At the end of nine months, the control seeds had shown 72 % damage and 39.67 % germination. In contrast, silver nanoparticles at 1000 ppm showed no seed damage and achieved 81.67 % germination, which was on par with copper nanoparticles at 1000 ppm with 79.33 % germination. Seed priming of silver and copper nanoparticles at 1000 ppm also demonstrated superior performance in all the seed quality and biochemical parameters (alpha amylase and catalase) throughout the storage period. Whereas, in the greenhouse experiment, enhanced growth (35.96 cm, 46.48 cm, and 53.00 cm at 30, 60 DAS, and at harvest, respectively) and yield per plant (3.75 g) were significantly higher in plants that were given foliar application with silver nanoparticles at 1000 ppm. Furthermore, foliar application of these nanoparticles at all concentrations (1000, 1500, and 2000 ppm) did not exhibit any adverse effects on soil microbial organisms, as assessed by dehydrogenase enzyme activity. Hence, this research highlights the potential use of silver and copper nanoparticles at 1000 ppm as effective tools for storage pest management and contributing to improved agricultural productivity and sustainability.

---

* Corresponding author.
  E-mail address: hemaagbsc@gmail.com (M. Hemalatha).

1. Introduction

Technology has been evolving since its inception by mankind. It has transformed to satisfy the most imminent necessities of human life. Every day perpetually adds more mouths to our population demanding an unhindered supply of food. Today, food security stands alongside every nation's national security, and it cannot be overlooked. Predictions show that food demand is likely to rise from 59 to 98 % for the world population, reaching 9 billion by 2050 [1]. Despite an increase in the world population, particularly in developing countries, the global food supply is interrupted by the expenditure of bio-resources for the production of energy, manufacturing chemicals, high post-farming losses, less value addition, inefficient distribution and marketing systems, and other factors [2]. We are experiencing "technology fatigue" in agriculture, which means we need to upgrade. It is high time that we seek the evolution of technology to strengthen our backbone, *i.e.*, agriculture.

One of the extremely promising 21st-century technologies that can potentially meet the demands of agriculture is nanotechnology, or nanotech in brief. It would be worth mentioning here that the European Commission has revered this technology as one of six "key enabling technologies" for sustainability in different areas [3]. Nanotechnology can play an important role in transforming agriculture by creating innovative solutions for sustainable food production. Nanotechnology has the potential to transform agriculture by creating innovative solutions that are more sustainable, efficient, and effective. However, it is important to ensure that the use of nanotechnology in agriculture is safe and environmentally friendly.

"Tiny is beautiful and tiny is potential" holds well in the case of nanoparticles. Nanoparticles, generally considered as particles with a size of up to 100 nm, exhibit completely new or improved properties as compared to the larger particles of the bulk material. In recent years, noble metal nanoparticles have become increasingly favored among researchers due to their significant physicochemical and biological attributes. Currently, various types of metal nanomaterials, including iron, silver, zinc, gold, copper, potassium, magnesium, alginate, and titanium, are being synthesized owing to their distinctive intrinsic properties and versatile applications in diverse fields such as biomedicine, environmental remediation, organic photovoltaics, sensors, optical imaging, and therapeutic agents. Furthermore, they find extensive use as catalysts in numerous chemical reactions [4].

Nanoparticles are synthesized using different techniques and, more commonly using the chemical reduction methods [5]. Since applications of nanoparticles (NPs) in agriculture need to be economical, eco-friendly, biocompatible, and non-toxic, the biological approach for the synthesis of nanoparticles becomes imperative [6]. Nanoparticle synthesis from biological sources like microorganisms, plant extracts, and enzymes is considered effective and provides eco-friendly alternatives to physical and chemical reduction methods. There are no harsh chemicals or media involved in the plant-mediated synthesis, making it virtually green. The NPs as synthesized also bear substantial inherent stability due to great dispersion [7]. Plant extracts are used for the bioreduction of metal ions to form nanoparticles. It has been demonstrated that plant metabolites like sugars, terpenoids, polyphenols, alkaloids, phenolic acids, and proteins play an important role in the reduction of metal ions into nanoparticles and support their subsequent stability.

According to the FAO, approximately 10–25 % of harvested food worldwide is destroyed annually by insects and rodent pests [8]. Grain damage arising from direct feeding of insects on grain endosperm and embryos increases the exposure of grain to rot, and fissures on seed lead to unpleasant odors that are not fit for human and animal consumption. Greengram (*Vigna radiata* L.) is the third most important pulse crop in India, covering an area of 4.74 m ha with a total production of 2.62 m tonnes and a productivity of 553 kg/ha [9]. Greengram serves as a cash crop for farmers and is an excellent source of digestible protein with low flatulence. Greengram contains about 24 per cent protein, which is comparatively rich in lysine, an amino acid deficient in cereal grains. So, a diet combining greengram and cereal grains forms a balanced amino acid diet [10]. The existing level of greengram production is lower than its potential. This is because it suffers both qualitative and quantitative losses due to the attack of storage pests. Due to inappropriate and inefficient storage methods, there is a substantial quantitative loss of around 7.5 per cent during storage [11].

Among the storage pests, bruchids are known to cause considerable loss. The genus *Callosobruchus* includes a number of economically significant species that attack stored pulses throughout the world. But *Callosobruchus maculatus* (Fabricus), *Callosobruchus chinensis* (Linnaeus), and *Callosobruchus analis* (Fabricus) are common species in India. Among them, *Callosobruchus chinensis* (L.) (pulse beetle) is the most common pest of greengram. Due to its short life cycle and high degree of reproductive cycles, losses caused by this beetle to the pulses have been estimated to the tune of 30–40 per cent in storage [12]. The control of stored grain pests relies mostly on broad-spectrum insecticides and fumigants. Unfortunately, this leads to the contamination of food with toxic residues and a rapid decline in germination [13]. Hence, the present study was designed with a novel, rapid, and cost-effective route for the synthesis of AgNPs and CuNPs using Ocimum leaf extract. Tulasi leaves have been traditionally used for the treatment of many infections. Its antibacterial activity has been reported to be the result of bioactive components, mostly eugenols. Silver nanoparticles (AgNPs) received much interest because of their strong surface plasmon resonance (SPR) property. Due to their antimicrobial and antioxidant properties, AgNPs were used in the coating for seed enhancement [14]. Copper nanoparticles (CuNPs) exhibited fungicidal and insecticidal activity against the pests of crop plants [15]. Several studies have reported the successful synthesis of silver (Ag) and copper (Cu) nanoparticles utilizing Ocimum leaf extract as a reducing and stabilizing agent [16,17]. These studies have highlighted the effectiveness of Ocimum leaf extract in producing nanoparticles with desired characteristics, including uniform size distribution and stability.

The synthesized AgNPs and CuNPs obtained by the green method were evaluated for their effect against pulse beetles in storage, quality, and yield aspects of greengram.

2. Materials and methods

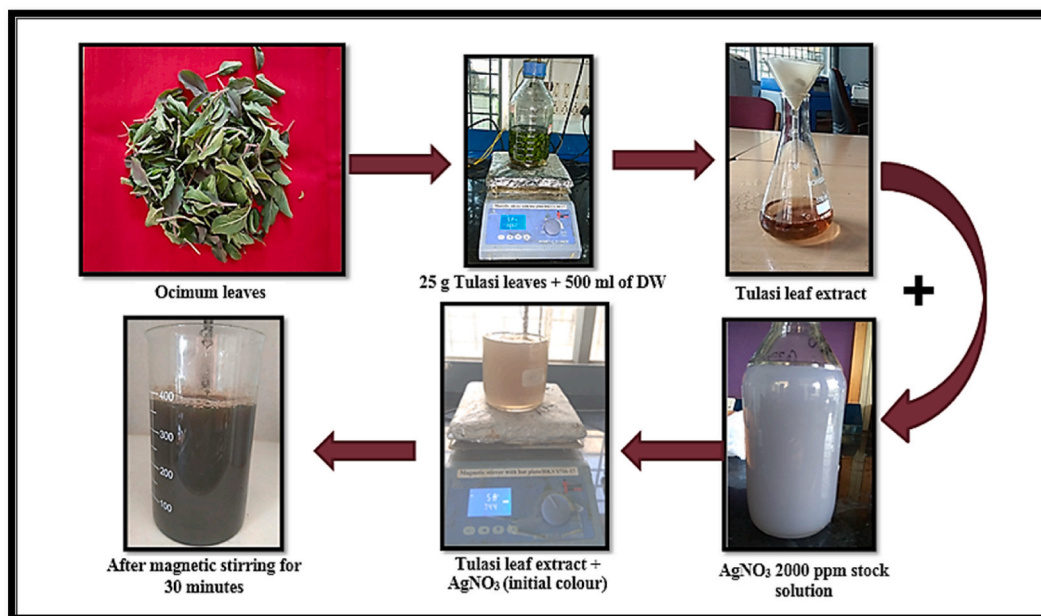### 2.1. Green synthesis of silver nanoparticles through ocimum leaf extract

Fresh leaves of ocimum were thoroughly washed under tap water to remove the dust, then washed with distilled water twice and dried at room temperature to remove moisture from the leaves. 25 g of ocimum leaves with 500 ml of distilled water were boiled for 30 min at 60 °C in a 1000 ml beaker. Leaf extract was cooled to room temperature and filtered with Whatman filter paper no. 1 and the filtrate was refrigerated at 4 °C for further use [18]. 2 g of silver nitrate ($AgNO_3$) was dissolved in 1000 ml of distilled water to get 2000 ppm of silver nitrate ($AgNO_3$) stock solution. For the synthesis of silver nanoparticles, freshly prepared 50 ml of $AgNO_3$ stock solution was added dropwise to 50 ml of ocimum leaf extract in a 1:1 ratio by continuous stirring on a magnetic stirrer at 60 °C for about 30 min. To confirm the formation of the AgNPs, bio-reduction of the silver ions in the medium was monitored by observing grey-black color (Fig. 1a). Later, the silver nanosolution was centrifuged at 10,000 rpm for 30 min at 4 °C. The supernatant was discarded, and pellets collected at the bottom of conical tubes were poured into the watch glass and placed in a hot air oven at 70 °C for 8 h. Later, powder from the watch glass was scraped and stored in vials under airtight condition for further use (Fig. 1b).

2.2. Green synthesis of copper nanoparticles through ocimum leaf extract

20 g of ocimum leaves with 200 ml of distilled water were boiled for 30 min at 60 °C in a 500 ml beaker. Leaf extract was cooled to room temperature and filtered with Whatman filter paper no. 1 and the filtrate was refrigerated at 4 °C for further use. 2.5 g of copper sulphate ($CuSO_4 \cdot 5H_2O$) was dissolved in 1 L of distilled water to get 2500 ppm of copper sulphate ($CuSO_4 \cdot 5H_2O$) stock solution. For the synthesis of copper nanoparticles, 10 ml of ocimum leaf extract was added dropwise to the freshly prepared 100 ml of $CuSO_4 \cdot 5H_2O$ stock solution in a 1:10 ratio by continuous stirring on a magnetic stirrer at 60 °C till there was change in color from light green to dark green (Fig. 2a). This color change indicates the formation of copper nanoparticles. Later, the copper nanosolution was centrifuged at 10000 rpm for 30 min at 4 °C. The supernatant was discarded, and pellets collected at the bottom of conical tubes were poured into the watch glass and placed in a hot air oven at 70 °C for 8 h. Later, powder from the watch glass was scraped and stored in vials under airtight condition for further use (Fig. 2b).

2.3. Characterization of green synthesized silver and copper nanoparticles

Green-synthesized silver and copper nanoparticles were characterized using a variety of analytical techniques. The confirmation of the reduction of Ag^+ and Cu^{2+} ions to Ag and Cu nanoparticles was achieved through UV–Vis spectrophotometry using a spectrophotometer (SP-UV 500DB, Germany). The wavelength range of 200–800 nm was scanned to identify the optical absorbance peak. To determine the average particle size, dynamic light scattering (DLS) was employed. This was conducted using a high-performance particle-size analyzer (model Z3000, Nicomp, USA). The subsequent step involved analyzing the surface morphology of the silver

Fig. 1a. Standardization of the protocol for green synthesis of silver nanoparticles from ocimum leaf extract. (For interpretation of the references to color in this figure legend, the reader is referred to the Web version of this article.)

Fig. 1b. Conversion of silver nanosolution into nanopowder.

Fig. 2a. Standardization of the protocol for green synthesis of copper nanoparticles from ocimum leaf extract. (For interpretation of the references to color in this figure legend, the reader is referred to the Web version of this article.)
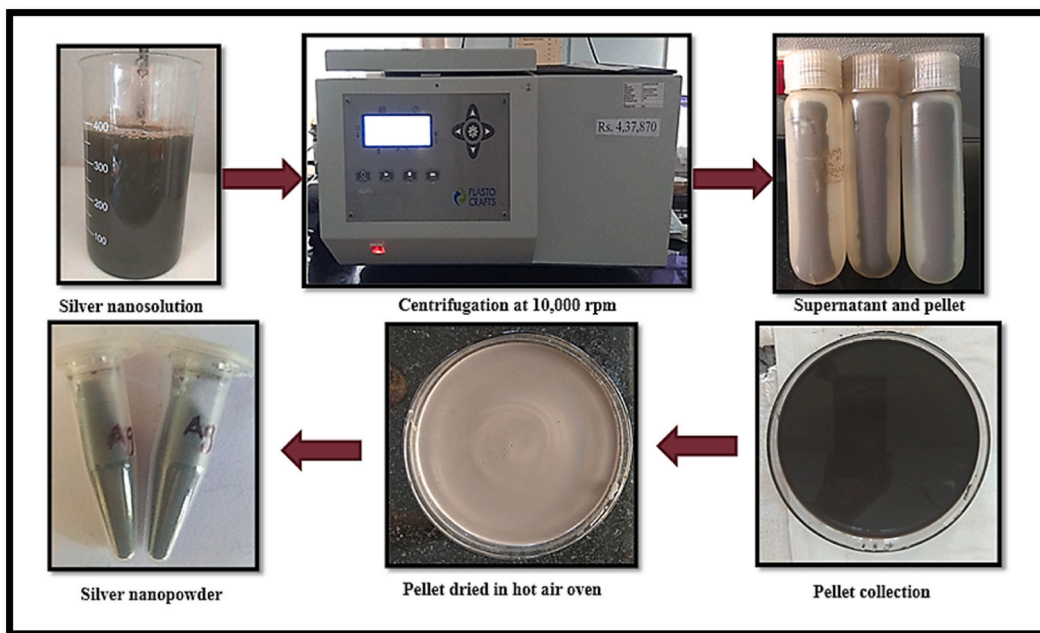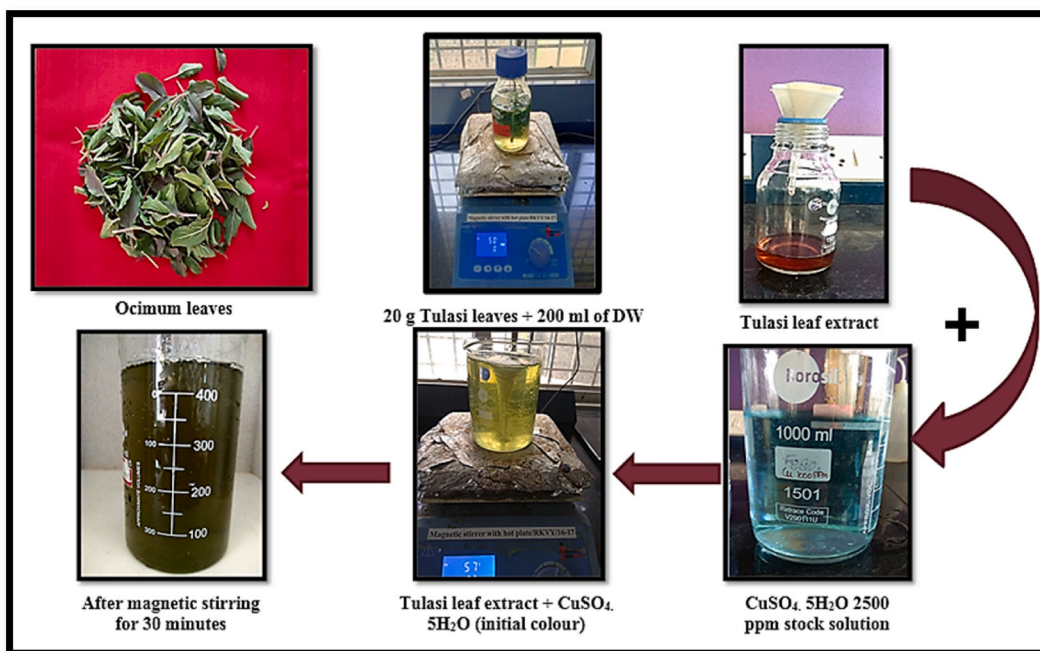
and copper nanoparticles using scanning electron microscopy (SEM) from Carl Zeiss, Germany. The presence of Ag^+ and Cu^{2+} ions was further validated using energy-dispersive X-ray spectroscopy (EDS), which was attached to the EVO 18 scanning electron microscope. To understand the crystalline structure, the reduced silver and copper nanoparticles were subjected to X-ray diffraction (XRD) analysis. This analysis was performed using the Rigaku TTR (Tokyo, Japan) at specific parameters. Functional groups in the samples were identified through Fourier-transform infrared (FTIR) analysis. The synthesized nanoparticles (AgNPs and CuNPs) powder was used for this purpose. FTIR spectrometry was conducted using a Thermo Nicolet Model 6700 spectrometer (Thermo Scientific, Waltham, MA,
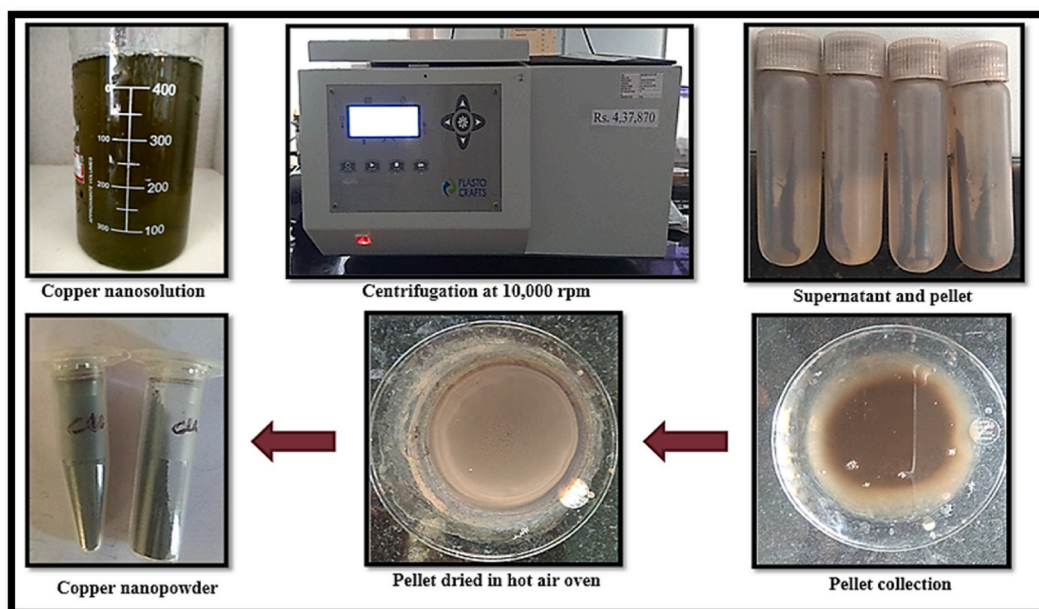
Fig. 2b. Conversion of copper nanosolution into nanopowder.

USA).

2.4. Seed priming and insect release

Seeds of the DGGV-2 greengram variety were subjected to priming with Ag and CuNPs solutions (at concentrations of 1000, 1500, and 2000 ppm). The priming process involved a seed-to-synthesized nanoparticles solution ratio of 1:2. In the case of AgNPs treatment, the priming duration was set at 3 h, while for CuNPs treatments, the priming time was 1 h, as previously determined by a preliminary experiment (based on seed quality test). The seeds were also treated with castor oil (10 ml/kg seed) and deltamethrin (0.04 ml/kg). Following this, the seeds were shade dried to bring down to safe moisture content. Later, 500 g of seeds for each replication were transferred to cloth bags of size 25 cm × 20 cm. In the laboratory, pulse beetles were reared on greengram within a glass jar. The jar was covered with a piece of muslin cloth and maintained at ambient temperature and relative humidity. Ten pairs of freshly emerged male and female pulse beetle adults collected from a well-maintained culture were released into the seed storage bags and kept for storage under ambient conditions. Observations on seed quality parameters and insect infestation parameters were recorded at monthly intervals up to nine months.

2.5. Greenhouse experiment

In greenhouse, the stored seeds were planted in pots, and foliar application with Ag and Cu nanoparticles was given at the vegetative and reproductive stages to study their effect on plant growth, yield, and seed quality of greengram.

2.6. Observations recorded in the lab during storage study

2.6.1. Seed quality parameters

2.6.1.1. Seed germination. The number of normal seedlings in each replication was counted at the end of 7th day, and the germination percentage was calculated and expressed in percentage as given by ISTA [19].

$$\text{Normal seedlings }(\%) = \frac{\text{Number of normal seedlings}}{\text{Total number of seeds}} \text{ X } 100$$

2.6.1.2. Root length. From the germination test, ten normal seedlings were selected randomly in each treatment from each replication on the 7th day. The root length was measured from the tip of the primary root to the base of hypocotyl, and mean root length was expressed in centimeters.

2.6.1.3. Shoot length. From the germination test, ten normal seedlings were selected randomly in each treatment from each replication

on 7th day. The shoot length was measured from the base of the primary leaf to base of hypocotyl, and mean shoot length was expressed in centimeters.

2.6.1.4. Seedling vigour index (SVI). Vigour index was computed by using the following formula and expressed in number [20].

Seedling vigour index = germination% × [shoot length (cm) + root length (cm)].

2.6.1.5. Seed infestation percentage. Three hundred seeds in each replication are taken at random from each treatment. The seeds were separated into damaged and undamaged categories. The damaged seeds were counted. Percentage seed damage was calculated as described by Ref. [21].

$$\text{Seed infestation \%} = \frac{\text{No. of pulse beetle damaged seeds}}{\text{Total no. of seeds observed}} \times 100$$

Morphological variations in insects collected from seeds treated with nanoparticles were observed under a stereomicroscope and compared with insects collected from control seeds.

2.6.2. Bio-chemical parameters in seed

2.6.2.1. Catalase activity. 0.5 g of greengram seeds were ground into fine powder in a pre-chilled mortar and pestle using ice cubes and homogenized in 2.0 ml of ice-cold extraction buffer of specific pH and molarity for each enzyme [22]. Catalase (CAT) was extracted in 0.05 M sodium phosphate buffer with a pH of 7.0. The enzyme homogenate was centrifuged at 14000 rpm for 20 min at 4 °C, and the supernatant maintained at 4 °C was used as enzyme source in the assay. The reaction mixture in the test cuvette contained 2.98 ml of 0.051 % substrate (hydrogen peroxide) in 50 mM, pH 7.0 phosphate buffer. It was read against a control cuvette containing 2.98 ml of H_2O_2 free phosphate buffer, 50 mM, pH 7.0 (Substrate blank was used because the enzyme extract absorbed strongly at 240 nm. Hence, to nullify the absorbance of the extract, it was introduced in both cuvettes). Buffer and substrate solutions were brought to 25 °C before assay. Control and test cuvettes were placed in a UV–Visible spectrophotometer and monitored at A_{240} for 5 min for stabilization, after which 0.02 ml of enzyme extract was added to both blank and test solutions. The solutions were mixed immediately by inversion. The decrease in absorbance was measured at 240 nm for up to 8 min. This procedure was standardized using a pure catalase enzyme from bovine liver (procured from Sigma Aldrich India) according to the method suggested by Beers and Sizer [23].

2.6.2.2. Alpha amylase activity. The activity of the α-amylase enzyme was estimated as per the procedure suggested by Lide and David [24], with minor modifications. A blank solution was prepared by adding 0.5 ml of substrate and 0.5 ml of phosphate buffer. The test solution was prepared by adding 0.5 ml of substrate and 0.5 ml of enzyme. The test and the blank solution were incubated for 5 min and 1 ml of DNSA was added to stop the reaction. The enzyme (0.5 ml) was added to the blank, and both the test and the blank were kept in a boiling water bath for 5 min. The volume was made up to 10 ml with distilled water, and the absorbance was recorded at 540 nm. By finding out the amount of maltose produced during the enzymatic reaction using a maltose calibration curve, the enzyme activity was calculated. The protein content of the enzyme source was calculated by FCR method. The specific activity of α-amylase was expressed as μg of maltose produced per minute per mg of protein.

2.7. Observations recorded in greenhouse conditions

2.7.1. Plant height (cm)
The height of five plants was measured from the base of the plant to tip of the plant, and average height of the plant was calculated on 30, 60 days, and at harvesting and expressed in centimeters.

2.7.2. Number of branches per plant
The number of primary and secondary branches was counted on 30, 60 days, and at harvesting period, and the total number of branches was counted from five randomly selected plants, and their mean was recorded as the number of branches per plant.

2.7.3. Days to 50 % flowering
The number of days taken for 50 % of plants in a pot to flower was recorded by counting the days from sowing to the date on which the 50 % of plants flower in the pot.

2.7.4. Number of pods per plant
The total number of pods produced per plant was counted among five randomly selected plants, and the average pods per plant were worked out.

2.7.5. Seed yield per plant (g plant^{-1})
The pods from five randomly selected plants were harvested, threshed, and weighed separately, and the average seed yield per plant was expressed in grams.

2.7.6. Dehydrogenase activity in soil

Dehydrogenase activity in the soil samples was determined as per the procedure described by Casida et al. [25]. Ten grams of soil and 0.2 g of $CaCO_3$ were thoroughly mixed and dispensed in test tubes. To each tube, one ml of a 3 per cent aqueous solution of 2,3, 5-triphenyl tetrazolium chloride (TTC), one ml of one per cent glucose solution, and eight ml of distilled water were added, which was sufficient to leave a thin film of water above the soil layer. The tubes were stoppered with rubber cork and incubated at 30 $^\circ$C for 24 h. At the end of incubation, the contents of the tube were rinsed down into a small beaker, and a slurry was made by adding 10 ml of methanol. The slurry was filtered through Whatman No. 50 filter paper. Repeated rinsing of the soil with one ml of methanol was continued till the filtrate ran free of red color. The filtrate was pooled and made up to 50 ml with methanol in a volumetric flask. The intensity of the red color was measured at 485 nm against a methanol blank using a spectrophotometer. The concentration of formazan in soil samples was determined by reference to a standard curve prepared by using graded concentrations of formazan. The results were expressed as triphenyl formazan (TPF) formed g^{-1} soil.

3. Results

3.1. Characterization of green synthesized silver and copper nanoparticles

The formation of nanoparticles was primarily indicated by a noticeable change in color. The confirmation of synthesized silver nanoparticles was based on the observation of a grey-black color, while the synthesis of copper nanoparticles was validated through the emergence of a dark green color.

3.1.1. UV–Visible spectroscopy

The utilization of ocimum leaves for the biosynthesis of silver nanoparticles, exhibited a prominent absorption peak at 475 nm (Fig. 3). Similarly, the biosynthesis of copper nanoparticles using ocimum leaves yielded a maximum absorption peak at 322 nm (Fig. 4).

3.1.2. Particle size analyzer (PSA)

The mean diameter of the synthesized AgNPs from ocimum leaf extract was 54.1 nm (Fig. 5). Whereas, 25 per cent of the mean diameter distribution was below 32.1 nm. Similarly, the mean diameter of the synthesized CuNPs from ocimum leaf extract was 74.9 nm (Fig. 6). Whereas, 25 per cent of the mean diameter distribution was below 42.9 nm.

3.1.3. Scanning electron microscope (SEM) and energy dispersive X-ray (EDX)

Examination of the silver nanoparticles synthesized using ocimum leaf extract, through SEM and EDX analysis, revealed their morphology as predominantly round to spherical (Fig. 7). The EDS spectral images displayed a distinct peak at 3 keV (Lα), which affirmed the presence of elemental silver (Ag). The pronounced peaks in the EDX data indicated that silver constituted 83.58 % of the composition (Fig. 8), serving as additional confirmation for the generation of pure silver nanoparticles. Similarly, the characterization of copper nanoparticles synthesized using ocimum leaf extract, employing SEM and EDX techniques, revealed their structure to be spherical (Fig. 9). Further EDX examination of the copper nanoparticles displayed a characteristic signal attributed to both copper and oxygen. The chemical composition analysis determined that copper accounted for 81.36 % of the material (Fig. 10), thus providing supplementary support for the creation of pure copper nanoparticles.

3.1.4. X-Ray diffraction (XRD)

AgNPs showed five main peaks of 32.23°, 38.10°, 44.34°, 64.58°, and 76.76° corresponding to (101), (111), (200), (220), and (311) lattice planes, respectively (Fig. 11). Whereas, the major peak positions at 2θ values of 35.61° (111) and 38.79° (200) in the high angle

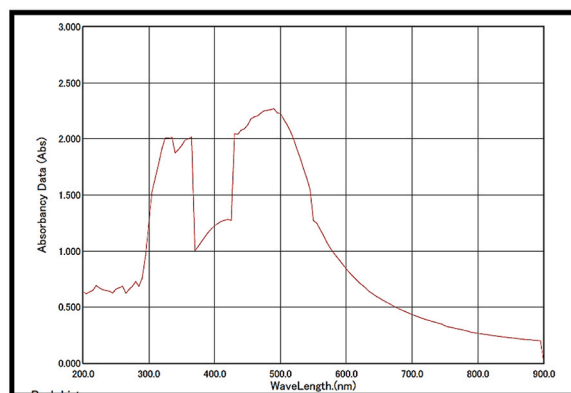**Fig. 3.** Characterization of synthesized AgNPs from tulasi leaf extract by UV-Vis spectrophotometer.
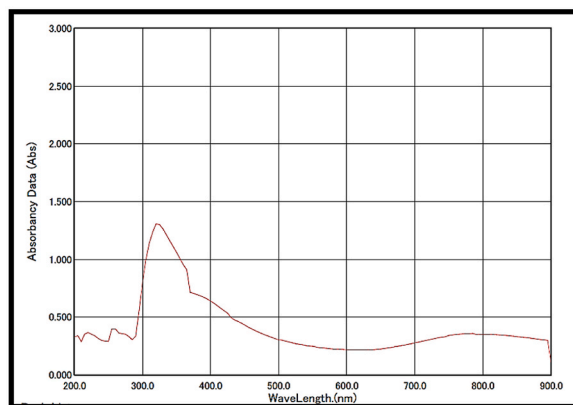
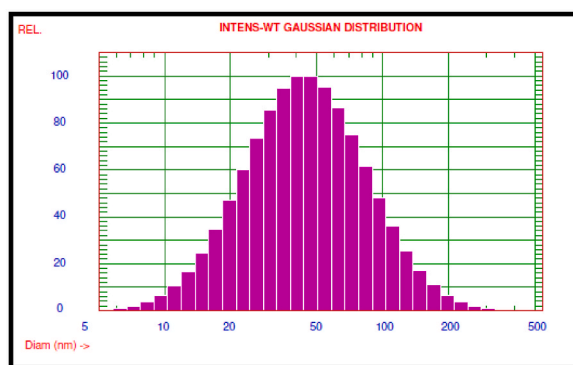**Fig. 4.** Characterization of synthesized CuNPs from tulasi leaf extract by UV-Vis spectrophotometer.

Fig. 5. Characterization of synthesized AgNPs from tulasi leaf extract by particle size analyzer (PSA).
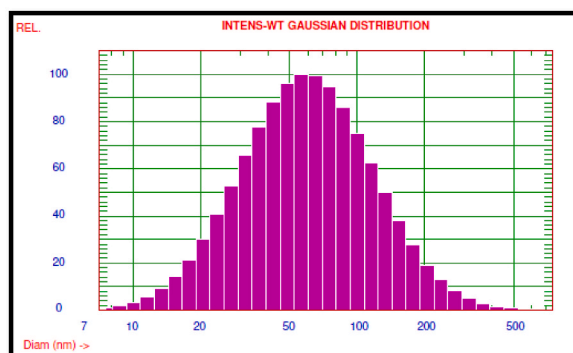

Fig. 6. Characterization of synthesized CuNPs from tulasi leaf extract by particle size analyzer (PSA).

XRD of copper nanoparticles indicate the existence of cubic centered crystalline nature of nanoparticles (Fig. 12). The mean crystallite size in case of AgNPs and CuNPs biosynthesized using ocimum leaf extract was calculated to be 25.67 nm and 34.83 nm respectively. The range of crystalline size for AgNPs was 14.68–47.09 nm and for CuNPs, the range was 20.45–55.17 nm. The sharp peaks in AgNPs and CuNPs sturdily designated the face centered cubic (fcc) symmetry and crystallinity.

3.1.5. Fourier transform infrared spectroscopy (FTIR)

FTIR analysis of silver nanoparticles biosynthesized through ocimum leaf extract revealed absorption peaks occurring at 3849, 3745, and 3676 corresponding to the hydroxyl (OH) groups, The peaks at 3047 cm^{-1}, 2839 cm^{-1}, and 2619 cm^{-1} correspond to symmetric CH$_2$ stretching and C–H aldehyde groups, respectively. The presence of nitrile and P–H ester stretching is indicated by the
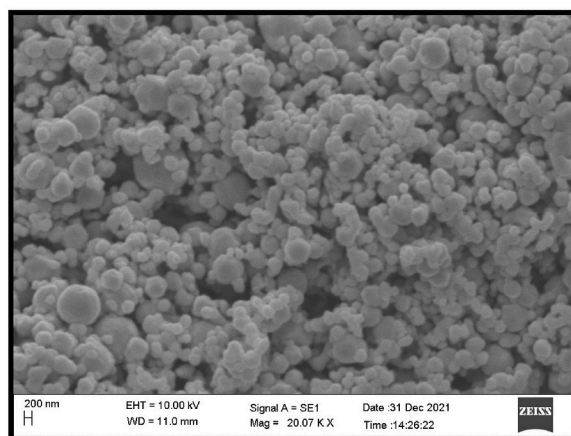
Fig. 7. Surface morphology of silver nanoparticles by scanning electron microscope.

Fig. 8. Elemental peaks and distribution of silver nanoparticles with energy-dispersive X-ray spectroscopy (EDX).
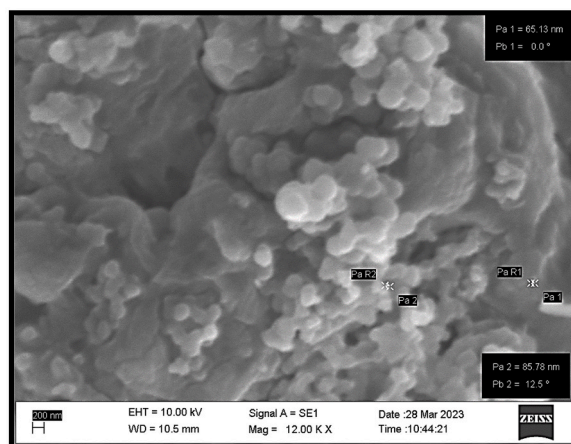
Fig. 9. Surface morphology of copper nanoparticles by scanning electron microscope.

peak at 2337 cm^{-1}. The peak at 2083 cm^{-1} corresponds to C–N stretching vibration. The peak at 1882 cm^{-1} indicates an aromatic group, while the peaks at 1581 cm^{-1} and 1342 cm^{-1} are attributed to C=N and C–N stretching of aromatic amine groups, respectively. The peaks at 1226 cm^{-1} and 1022 cm^{-1} correspond to C–N stretching of amines and -C-O-C- stretching, respectively. The peak at 802 cm^{-1} corresponds to aromatics, and the peak at 505 cm^{-1} indicates -C-I- stretching (alkyl halide) (Fig. 13). Similarly, FTIR analysis of copper nanoparticles biosynthesized through ocimum leaf extract revealed absorption peaks occurring at 1593 cm^{-1}, which is indicative of the presence of the C=N functional group. The peak at 1519 cm^{-1} can be attributed to the N–H bond bending
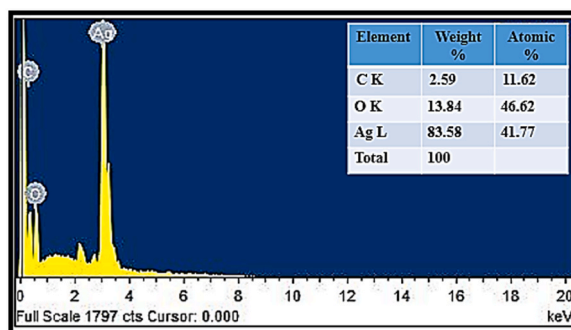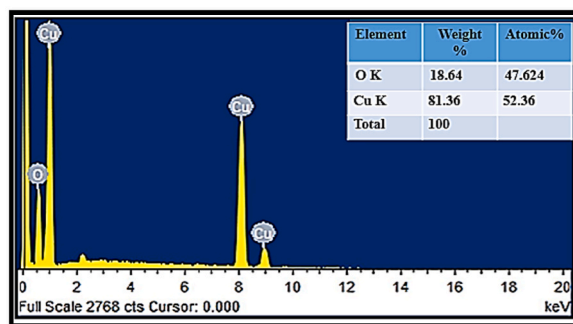
Fig. 10. Elemental peaks and distribution of silver nanoparticles with energy-dispersive X-ray spectroscopy (EDX).
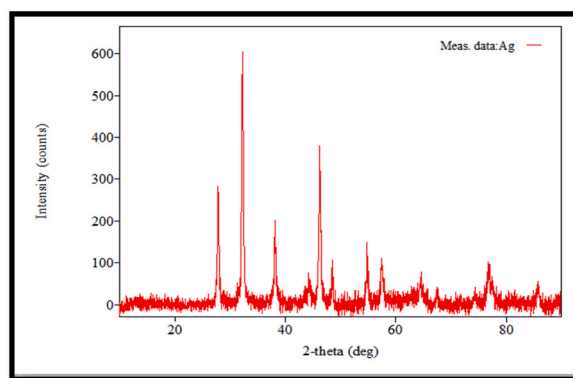
**Fig. 11.** Diffraction pattern of biosynthesized silver nanoparticles by X-ray diffraction (XRD).
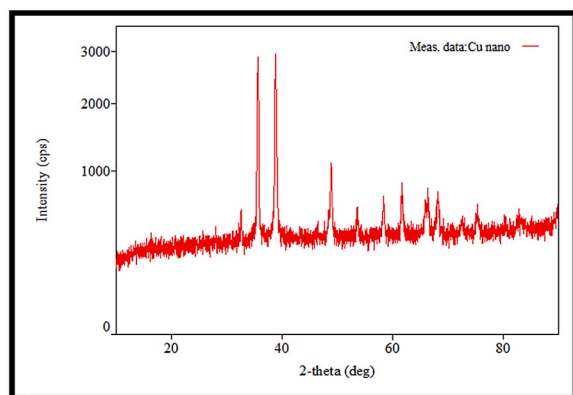
Fig. 12. Diffraction pattern of biosynthesized silver nanoparticles by X-ray diffraction (XRD).

characteristic of an amine group. The appearance of the peak at 1427 cm^{-1} is associated with the C–C stretching of an aromatic ring structure. Peaks at 1361 cm^{-1} and 1354 cm^{-1} are related to the C–N stretching of amide functional groups. The presence of the peak at 1072 cm^{-1} signifies C–N stretching vibrations of aliphatic amines. The peak at 771 cm^{-1} indicates C–H stretching. Additionally, the peak at 597 cm^{-1} corresponds to bending modes of vibrations involving the C–H bond, and the peak at 459 cm^{-1} corresponds to the C–Cl functional group (Fig. 14).
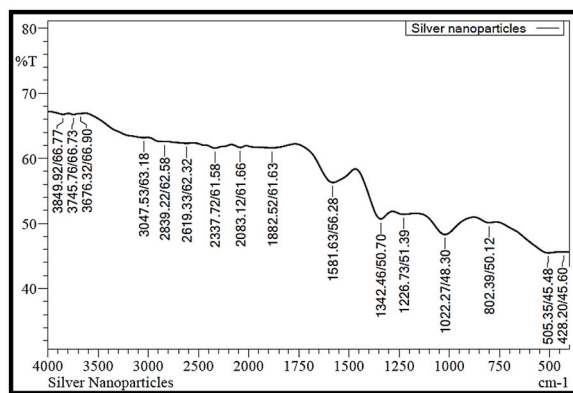
Fig. 13. Fourier transform infrared spectroscopy (FTIR) images of biosynthesized silver nanoparticles.
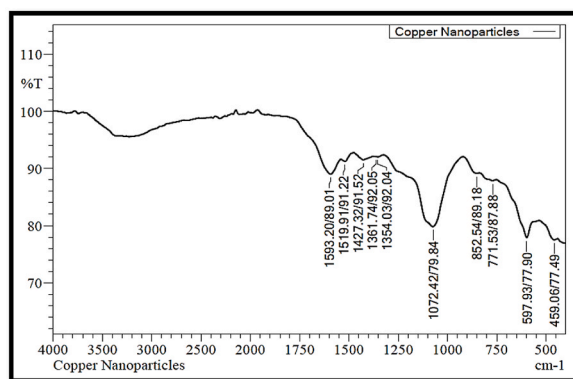
Fig. 14. Fourier transform infrared spectroscopy (FTIR) images of biosynthesized copper nanoparticles.

3.2. Influence of biosynthesized silver and copper nanoparticles against pulse beetles and on seed quality parameters of greengram during storage under lab conditions

3.2.1. Seed germination

The results, as influenced by the nanopriming with silver and copper nanoparticles biosynthesized using ocimum leaf extract, on the seed germination of greengram seeds at different months of storage, are presented in Table 1.

In the initial month of storage, the higher germination percentage was significantly observed in seeds primed with AgNPs at 1000 ppm (T_1-96.00 %) when compared to rest of the treatments, but was on par with the results of CuNPs at 1000 ppm (T_4-94.67 %) and AgNPs at 1500 ppm (T_2-94.33 %). Conversely, control (T_9-88.33 %) exhibited significantly the lower germination percentage, which was on par with CuNPs at 2000 ppm (T_6-89.33 %). At the end of the ninth month, significantly higher seed germination was observed in seeds primed with AgNPs at 1000 ppm (T_1-81.67 %), on par with CuNPs at 1000 ppm (T_4-79.33 %). While significantly lower germination percentage was recorded in control (T_9-39.67 %). Seeds primed with AgNPs at a concentration of 1000 ppm exhibited the least reduction in germination percentage, recording only 14.93 % over the period from the first month to nine months of storage, in comparison to the other treatments.

3.2.2. Root length

The data on root length of greengram seeds as affected by nanopriming with silver and copper nanoparticles, synthesized using ocimum leaf extract, at various months of storage are given in Table 2.

During the initial month of storage, root length as influenced by the seeds nanoprimed with AgNPs varied significantly at a concentration of 1000 ppm (T_1-15.50 cm), which was on par with CuNPs at 1000 ppm (T_4-15.43 cm) and AgNPs at 1500 ppm (T_2-15.37 cm). Conversely, the control group (T_9) and seeds primed with CuNPs at 2000 ppm (T_6) displayed the least root length, with values of 14.63 cm and 14.83 cm, respectively. At the end of ninth month, significantly superior root length was observed in seeds primed with AgNPs at 1000 ppm (T_1-12.97 cm), which was on par with CuNPs at 1000 ppm (T_4-12.77 cm) and the lower root length was significantly recorded in control (T_9-8.67 cm).

Table 1

Effect of seed priming with AgNPs and CuNPs on germination (%) of greengram cv. DGGV-2 assessed at various post storage conditions under ambient environment.

Treatments	Months after storage									% Reduction over 1st month
	1	2	3	4	5	6	7	8	9	
T_1	96.00	95.00	93.67	92.33	91.67	89.00	86.33	83.00	81.67	14.93
	(78.52)	(77.12)	(75.23)	(73.95)	(73.23)	(70.67)	(68.34)	(65.66)	(64.66)	
T_2	94.33	93.33	91.33	89.00	88.00	85.33	82.33	79.33	77.67	17.66
	(76.31)	(75.05)	(72.88)	(70.63)	(69.73)	(67.48)	(65.15)	(62.96)	(61.80)	
T_3	91.33	89.00	87.33	83.67	82.00	80.33	76.00	72.67	70.33	22.99
	(72.88)	(70.67)	(69.17)	(66.17)	(64.91)	(63.68)	(60.68)	(58.48)	(57.00)	
T_4	94.67	94.33	92.67	91.00	90.00	87.67	85.00	81.00	79.33	16.20
	(76.70)	(76.31)	(74.30)	(72.56)	(71.57)	(69.44)	(67.22)	(64.16)	(62.97)	
T_5	91.00	88.33	87.00	84.33	81.33	78.00	75.33	72.33	69.33	23.81
	(72.56)	(70.03)	(68.90)	(66.69)	(64.41)	(62.03)	(60.22)	(58.27)	(56.37)	
T_6	89.33	87.33	85.00	82.00	79.67	75.67	71.67	68.00	64.33	27.99
	(70.94)	(69.15)	(67.22)	(64.90)	(63.22)	(60.46)	(57.84)	(55.55)	(53.33)	
T_7	91.67	90.00	88.67	85.67	83.00	80.33	77.33	73.33	71.00	22.55
	(73.25)	(71.58)	(70.33)	(67.79)	(65.66)	(63.69)	(61.57)	(58.92)	(57.42)	
T_8	93.00	91.67	90.00	87.33	86.67	84.00	81.33	77.33	75.33	19.00
	(74.66)	(73.23)	(71.58)	(68.60)	(68.00)	(66.44)	(64.42)	(61.60)	(60.23)	
T_9	88.33	85.67	84.33	79.00	74.33	69.33	60.67	51.00	39.67	55.09
	(70.03)	(67.76)	(66.54)	(62.73)	(59.57)	(56.39)	(51.16)	(45.57)	(39.03)	
S.Em ($\pm$)	0.54	0.55	0.58	0.61	0.59	0.62	0.68	0.60	0.65	–
C.D (1 %)	2.22	2.25	2.35	2.49	2.40	2.54	2.78	2.45	2.64	–
C.V.	1.27	1.32	1.41	1.55	1.53	1.68	1.91	1.76	1.98	–

*Figures in the parentheses indicate arcsine root transformed values.
Treatment details:
T_1: AgNPs at 1000 ppm T_4: CuNPs at 1000 ppm T_7: Castor oil @ 10 ml/kg.
T_2: AgNPs at 1500 ppm T_5: CuNPs at 1500 ppm T_8: Deltamethrin @ 0.04 ml/kg.
T_3: AgNPs at 2000 ppm T_6: CuNPs at 2000 ppm T_9: Control (untreated).

Table 2

Effect of seed priming with AgNPs and CuNPs on root length (cm) of greengram cv. DGGV-2 assessed at various post storage conditions under ambient environment.

Treatments	Months after storage								
	1	2	3	4	5	6	7	8	9
T_1	15.50	15.43	15.33	14.87	14.63	14.20	13.93	13.57	12.97
T_2	15.37	15.30	15.20	14.43	14.07	13.43	13.13	12.63	11.87
T_3	15.07	14.73	14.53	13.87	13.23	12.40	12.03	11.50	10.63
T_4	15.43	15.40	15.27	14.77	14.47	14.00	13.77	13.40	12.77
T_5	15.00	14.73	14.60	13.83	13.20	12.10	11.97	11.47	10.60
T_6	14.83	14.60	14.47	13.57	12.87	11.73	11.23	10.53	9.63
T_7	15.10	14.97	14.80	14.00	13.33	12.53	12.13	11.53	10.73
T_8	15.17	15.07	14.93	14.30	13.90	13.23	12.90	12.47	11.80
T_9	14.63	14.40	14.20	13.20	13.20	12.40	11.07	10.47	9.60	8.67
S.Em ($\pm$)	0.06	0.08	0.08	0.09	0.11	0.15	0.17	0.23	0.23
C.D (1 %)	0.26	0.32	0.31	0.36	0.43	0.63	0.69	0.92	0.94
C.V.	0.73	0.91	0.89	1.08	1.35	2.10	2.38	3.29	3.63

Treatment details:
T_1: AgNPs at 1000 ppm T_4: CuNPs at 1000 ppm T_7: Castor oil @ 10 ml/kg.
T_2: AgNPs at 1500 ppm T_5: CuNPs at 1500 ppm T_8: Deltamethrin @ 0.04 ml/kg.
T_3: AgNPs at 2000 ppm T_6: CuNPs at 2000 ppm T_9: Control (untreated).

3.2.3. Shoot length

The results depicting the impact of nanopriming with silver and copper nanoparticles, synthesized using ocimum leaf extract on the shoot length of greengram seeds at various months of storage are presented in Table 3.

Significant variation on shoot length was recorded in seeds primed with AgNPs at 1000 ppm (T_1-25.47 cm), on par with CuNPs at 1000 ppm (T_4-25.40 cm) and AgNPs at 1500 ppm (T_2-25.33 cm), whereas control seeds (T_9-24.37 cm) exhibited significantly the least shoot length when compared to all the treatments but had shown on par with the seeds primed with CuNPs at 2000 ppm (T_6-24.40 cm) at the end of the first month of storage. At the end of the ninth month, significantly higher shoot length was observed in seeds primed with AgNPs at 1000 ppm (T_1-21.87 cm), which was on par with CuNPs at 1000 ppm (T_4-21.63 cm). The lower shoot length with a significant decline was recorded in control (T_9-16.87 cm).

Table 3
Effect of seed priming with AgNPs and CuNPs on shoot length (cm) of greengram cv. DGGV-2 assessed at various post storage conditions under ambient environment.

Treatments	Months after storage								
	1	2	3	4	5	6	7	8	9
T_1	25.47	25.40	25.33	25.20	24.97	23.97	23.03	22.93	21.87
T_2	25.33	25.27	25.13	24.47	24.20	23.13	22.13	21.87	20.77
T_3	24.83	24.40	23.97	23.53	23.00	21.97	20.97	20.67	19.23
T_4	25.40	25.33	25.23	25.00	24.70	23.80	22.90	22.80	21.63
T_5	24.83	24.40	23.93	23.43	22.93	21.87	20.93	20.60	19.10
T_6	24.40	24.20	23.77	23.00	22.40	21.17	20.03	19.57	18.00
T_7	24.87	24.73	24.50	23.73	23.17	22.10	21.10	20.73	19.37
T_8	25.00	24.87	24.60	24.27	23.93	22.93	22.00	21.77	20.53
T_9	24.37	23.93	23.30	22.26	21.63	20.37	19.17	18.53	16.87
S.Em ($\pm$)	0.11	0.11	0.15	0.17	0.18	0.19	0.20	0.24	0.26
C.D (1 %)	0.44	0.45	0.60	0.70	0.72	0.78	0.83	0.99	1.08
C.V.	0.74	0.78	1.04	1.26	1.30	1.48	1.64	2.00	2.32

Treatment details:

T_1: AgNPs at 1000 ppm T_4: CuNPs at 1000 ppm T_7: Castor oil @ 10 ml/kg.

T_2: AgNPs at 1500 ppm T_5: CuNPs at 1500 ppm T_8: Deltamethrin @ 0.04 ml/kg.

T_3: AgNPs at 2000 ppm T_6: CuNPs at 2000 ppm T_9: Control (untreated).

3.2.4. Seedling vigour index-I

The influence on seedling vigour index-I of greengram seeds by nanopriming with silver and copper nanoparticles, synthesized using ocimum leaf extract, at various months of storage is given in Table 4.

Significant effect on seedling vigour index-I was observed in seeds nanoprimed with AgNPs at a concentration of 1000 ppm (T_1-3933) which was on par with CuNPs at 1000 ppm (T_4-3866) and AgNPs at 1500 ppm (T_2-3840) and significantly superior to all other treatments. In contrast, the significantly lower seedling vigour index-I was reported in the control group (T_9-3445) and it was on par with the seeds primed with CuNPs at 2000 ppm (T_6-3505) during the first month of storage. By the end of the ninth month, seeds primed with AgNPs at 1000 ppm (T_1-2845) exhibited a significantly higher seedling vigour index-I, which was on par with CuNPs at 1000 ppm (T_4-2729), while the control (T_9-1013) recorded lower seedling vigour index-I with significant variance. The per cent reduction of SVI-I from first month to nine months of storage was found to be lower (27.66 %) in seeds primed with AgNPs at 1000 ppm.

3.2.5. Seed infestation percentage

The impact on seed infestation in greengram seeds at different months of storage is affected by nanopriming with silver and copper nanoparticles, synthesized using ocimum leaf extract, as presented in Table 5.

A significant decrease in seed infestation was observed in the seeds primed with AgNPs and CuNPs at all concentrations (1000, 1500, and 2000 ppm) compared to the control group. Throughout the storage period, seeds nanoprimed with AgNPs and CuNPs showed no seed infestation. In contrast, the control group exhibited a gradual increase in mean seed infestation as the storage period advanced.

Table 4
Effect of seed priming with AgNPs and CuNPs on seedling vigour index-I of greengram cv. DGGV-2 assessed at various post storage conditions under ambient environment.

Treatments	Months after storage									% Reduction over 1st month
	1	2	3	4	5	6	7	8	9	
T_1	3933	3879	3809	3700	3630	3397	3193	3030	2845	27.66
T_2	3840	3786	3684	3462	3367	3121	2904	2737	2534	34.01
T_3	3644	3483	3363	3129	2971	2761	2508	2338	2101	42.34
T_4	3866	3842	3753	3619	3525	3314	3117	2932	2729	29.41
T_5	3625	3457	3353	3143	2939	2649	2479	2319	2059	43.20
T_6	3505	3388	3250	2998	2810	2490	2241	2047	1777	49.30
T_7	3664	3573	3485	3233	3030	2782	2570	2366	2137	41.68
T_8	3736	3661	3558	3368	3279	3038	2838	2648	2435	34.82
T_9	3445	3284	3163	2801	2530	2179	1798	1436	1013	70.60
S.Em ($\pm$)	34.38	35.02	39.62	42.25	43.69	47.83	53.40	55.10	55.83	–
C.D (1 %)	140	143	161	172	178	195	217	224	227	–
C.V.	1.61	1.69	1.97	2.24	2.43	2.90	3.52	3.93	4.43	–

Treatment details:

T_1: AgNPs at 1000 ppm T_4: CuNPs at 1000 ppm T_7: Castor oil @ 10 ml/kg.

T_2: AgNPs at 1500 ppm T_5: CuNPs at 1500 ppm T_8: Deltamethrin @ 0.04 ml/kg.

T_3: AgNPs at 2000 ppm T_6: CuNPs at 2000 ppm T_9: Control (untreated).

Table 5
Effect of seed priming with AgNPs and CuNPs on seed damage percentage (%) of greengram cv. DGGV-2 assessed at various post storage conditions under ambient environment.

Treatments	Months after storage								
	1	2	3	4	5	6	7	8	9
T_1	0.00 (0.71)	0.00 (0.71)	0.00 (0.71)	0.00 (0.71)	0.00 (0.71)	0.00 (0.71)	0.00 (0.71)	0.00 (0.71)	0.00 (0.71)
T_2	0.00 (0.71)	0.00 (0.71)	0.00 (0.71)	0.00 (0.71)	0.00 (0.71)	0.00 (0.71)	0.00 (0.71)	0.00 (0.71)	0.00 (0.71)
T_3	0.00 (0.71)	0.00 (0.71)	0.00 (0.71)	0.00 (0.71)	0.00 (0.71)	0.00 (0.71)	0.00 (0.71)	0.00 (0.71)	0.00 (0.71)
T_4	0.00 (0.71)	0.00 (0.71)	0.00 (0.71)	0.00 (0.71)	0.00 (0.71)	0.00 (0.71)	0.00 (0.71)	0.00 (0.71)	0.00 (0.71)
T_5	0.00 (0.71)	0.00 (0.71)	0.00 (0.71)	0.00 (0.71)	0.00 (0.71)	0.00 (0.71)	0.00 (0.71)	0.00 (0.71)	0.00 (0.71)
T_6	0.00 (0.71)	0.00 (0.71)	0.00 (0.71)	0.00 (0.71)	0.00 (0.71)	0.00 (0.71)	0.00 (0.71)	0.00 (0.71)	0.00 (0.71)
T_7	0.00 (0.71)	0.00 (0.71)	0.00 (0.71)	0.00 (0.71)	0.00 (0.71)	0.00 (0.71)	0.00 (0.71)	0.00 (0.71)	0.00 (0.71)
T_8	0.00 (0.71)	0.00 (0.71)	0.00 (0.71)	0.00 (0.71)	0.00 (0.71)	0.00 (0.71)	0.00 (0.71)	0.00 (0.71)	0.00 (0.71)
T_9	3.67 (2.04)	7.00 (2.73)	13.33 (3.72)	19.67 (4.49)	27.33 (5.27)	38.67 (6.26)	49.00 (7.03)	61.67 (7.88)	72.00 (8.51)
S.Em ($\pm$)	0.03	0.04	0.04	0.04	0.05	0.04	0.06	0.05	0.05
C.D (1 %)	0.11	0.14	0.16	0.18	0.19	0.18	0.25	0.20	0.21
C.V.	5.64	6.54	6.53	6.79	6.53	5.75	5.88	5.66	5.47

*Figures in the parentheses indicate square root transformed values.
Treatment details:
T_1: AgNPs at 1000 ppm T_4: CuNPs at 1000 ppm T_7: Castor oil @ 10 ml/kg.
T_2: AgNPs at 1500 ppm T_5: CuNPs at 1500 ppm T_8: Deltamethrin @ 0.04 ml/kg.
T_3: AgNPs at 2000 ppm T_6: CuNPs at 2000 ppm T_9: Control (untreated).

During the first month of storage, the control group (T_9-3.67 %) had the higher seed infestation percentage compared to all other treatments, while all treatments involving seeds primed with AgNPs and CuNPs (1000, 1500, and 2000 ppm), as well as seeds treated with castor oil at 10 ml/kg and deltamethrin at 0.04 ml/kg, showed no seed infestation (nil). This pattern persisted throughout the storage period. At the end of the nine-month storage period, the control group (T_9-72 %) exhibited the higher seed infestation with significant variation. On the other hand, all other treatments resulted in minimal seed infestation, with zero per cent damage to the seeds by the end of the storage study.

3.2.6. Catalase activity (μ mol of H_2O_2 decomposed/min/mg of protein)

The observations on the catalase activity of greengram seeds at different months of storage, as affected by nanopriming with silver and copper nanoparticles, synthesized using ocimum leaf extract, are presented in Table 6.

In the initial month of storage, seeds primed with AgNPs at 1000 ppm (T_1-0.864 μ mol of H_2O_2 decomposed/min/mg of protein) exhibited the higher catalase activity, which was significantly higher than the other treatments. But, CuNPs at 1000 ppm (T_4-0.853 μ mol of H_2O_2 decomposed/min/mg of protein) and AgNPs at 1500 ppm (T_2-0.846 μ mol of H_2O_2 decomposed/min/mg of protein) showed on par with AgNPs at 1000 ppm. In contrast, the control (T_9-0.782 μ mol of H_2O_2 decomposed/min/mg of protein) displayed significantly lower catalase activity, which was on par with CuNPs at 2000 ppm (T_6-0.799 μ mol of H_2O_2 decomposed/min/mg of protein). At the end of the ninth month, significantly higher catalase activity was observed in seeds primed with AgNPs at 1000 ppm (T_1-0.682 μ mol of H_2O_2 decomposed/min/mg of protein), on par with CuNPs at 1000 ppm (T_4-0.665 μ mol of H_2O_2 decomposed/min/mg of protein) and found significant to rest of all the treatments. While the significantly lower catalase activity was recorded in control

Table 6
Effect of seed priming with AgNPs and CuNPs on catalase activity (μ mol of H_2O_2 decomposed/min/mg of protein) assessed at various post storage conditions under ambient environment.

Treatments	Months after storage									% Reduction over 1st month
	1	2	3	4	5	6	7	8	9	
T_1	0.864	0.837	0.806	0.786	0.765	0.735	0.727	0.700	0.682	21.06
T_2	0.846	0.818	0.783	0.748	0.727	0.697	0.687	0.657	0.632	25.30
T_3	0.818	0.772	0.738	0.701	0.668	0.625	0.613	0.582	0.556	32.03
T_4	0.853	0.825	0.795	0.770	0.755	0.713	0.704	0.685	0.665	22.04
T_5	0.815	0.775	0.737	0.690	0.655	0.617	0.606	0.576	0.548	32.76
T_6	0.799	0.764	0.726	0.678	0.640	0.586	0.566	0.532	0.500	37.42
T_7	0.822	0.791	0.754	0.713	0.678	0.636	0.624	0.599	0.568	30.90
T_8	0.835	0.799	0.767	0.735	0.717	0.674	0.664	0.641	0.617	26.11
T_9	0.782	0.748	0.710	0.644	0.601	0.547	0.525	0.489	0.451	42.33
S.Em ($\pm$)	0.005	0.006	0.006	0.008	0.009	0.009	0.010	0.010	0.012	–
C.D (1 %)	0.020	0.023	0.026	0.034	0.035	0.037	0.039	0.041	0.047	–
C.V.	1.05	1.24	1.46	2.01	2.15	2.43	2.62	2.87	3.48	–

Treatment details:
T_1: AgNPs at 1000 ppm T_4: CuNPs at 1000 ppm T_7: Castor oil @ 10 ml/kg.
T_2: AgNPs at 1500 ppm T_5: CuNPs at 1500 ppm T_8: Deltamethrin @ 0.04 ml/kg.
T_3: AgNPs at 2000 ppm T_6: CuNPs at 2000 ppm T_9: Control (untreated).

(T$_9$-0.451 µ mol of H$_2$O$_2$ decomposed/min/mg of protein).

3.2.7. α-Amylase activity (µ mol/min/mg of protein)

The data representing the α-amylase activity of greengram seeds at various storage periods, influenced by nanopriming with silver and copper nanoparticles synthesized using ocimum leaf extract, can be observed in Fig. 16.

In the initial month of storage, seeds primed with AgNPs at 1000 ppm (T$_1$-0.0168 µ mol/min/mg of protein) exhibited the higher α-amylase activity, which was on par with CuNPs at 1000 ppm (T$_4$-0.0165 µ mol/min/mg of protein) and AgNPs at 1500 ppm (T$_2$-0.0164 µ mol/min/mg of protein). In contrast, the control (T$_9$-0.0149 µ mol/min/mg of protein) displayed significantly lower α-amylase activity, which was on par with CuNPs at 2000 ppm (T$_6$-0.0151 µ mol/min/mg of protein). At the end of the ninth month, seeds primed with AgNPs at 1000 ppm (T$_1$-0.0125 µ mol/min/mg of protein) showed significantly higher α-amylase activity, on par with CuNPs at 1000 ppm (T$_4$-0.0121 µ mol/min/mg of protein). While significantly lower α-amylase activity was recorded in control (T$_9$-0.0063 µ mol/min/mg of protein).

A decline in all the seed quality parameters and biochemical parameters with increasing concentrations of AgNPs and CuNPs was observed. AgNPs at 2000 ppm, CuNPs at 1500 ppm, and CuNPs at 2000 ppm showed lower germination percentage, shoot length, root length, seedling vigour index-I, catalase activity, and alpha amylase activity throughout the storage period compared to their lower concentrations, as well as compared to the seeds treated with castor oil and deltamethrin.

3.3. Influence of biosynthesized silver and copper nanoparticles on plant growth and seed yield of greengram under protected conditions

The primed seeds with AgNPs and CuNPs, as well as the seeds treated with castor and deltamethrin that were previously subjected to storage and used in the previous experiment, were transferred to pots. Foliar applications of AgNPs and CuNPs were given at the vegetative and flowering stages and evaluated for their impact on plant growth, yield, and seed quality under protected conditions. However, during the storage study, the control seeds experienced severe infestation, rendering them unusable. Therefore, stored untreated seeds were used as a substitute to serve as the control group.

3.3.1. Plant height (cm)

The mean data on plant height at 30, 60 DAS (days after sowing), and at harvest, as influenced by nanopriming and foliar application with silver and copper nanoparticles synthesized using ocimum leaf extract, is reported in Table 7.

Throughout various stages of plant growth, significant differences in plant height were consistently observed among the different treatments. Seeds that underwent nanopriming and foliar spraying with AgNPs at a concentration of 1000 ppm displayed the higher plant height, regardless of the plant's age (30, 60 DAS, and at harvest) (T$_1$-35.96 cm, 46.48 cm, and 53.00 cm, respectively), followed by seeds that were primed and foliar sprayed with CuNPs at 1000 ppm (T$_4$-34.78 cm, 44.00 cm, and 50.10 cm, respectively). On the other hand, the control group had significantly lower plant height at 30, 60 DAS, and at harvest (T$_9$-30.56 cm, 34.67 cm, and 39.00 cm, respectively).
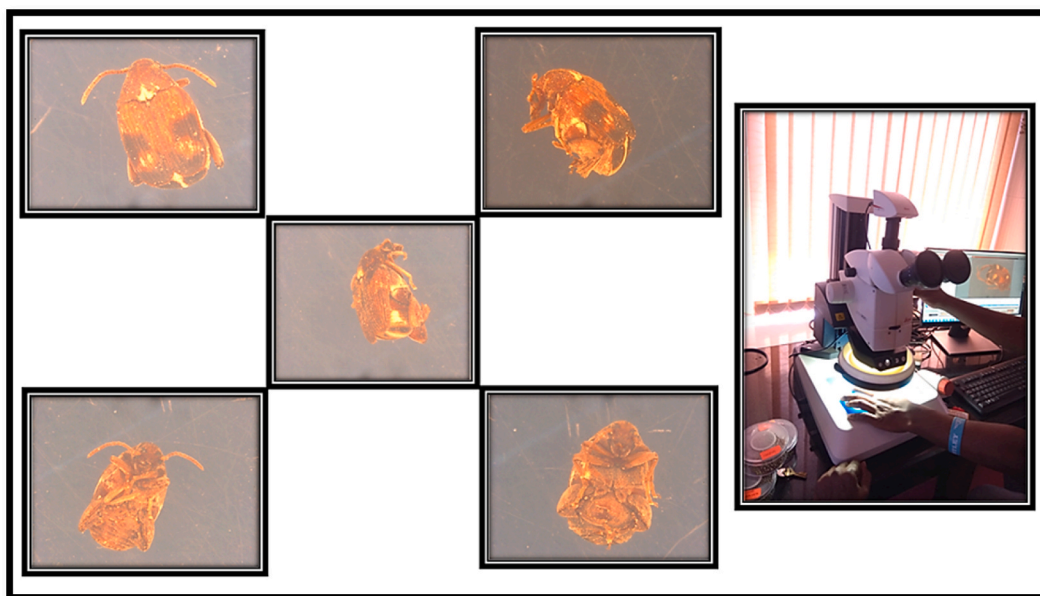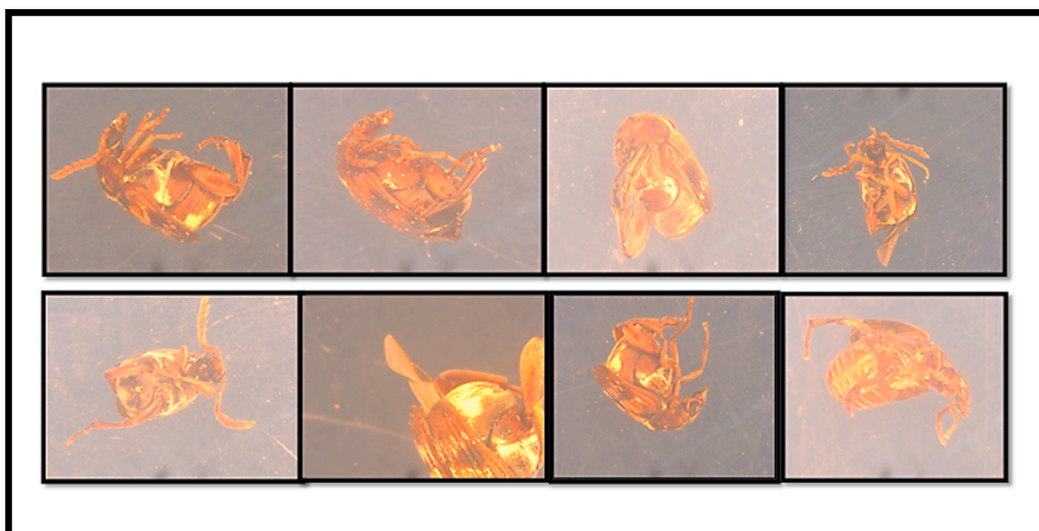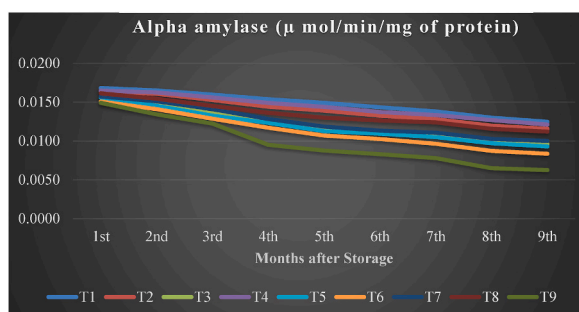

Fig. 15a. Stereomicroscopic images of pulse beetles in control treatment.

Fig. 15b. Morphological variations observed in pulse beetle due to AgNPs and CuNPs treatment in seeds.

Fig. 16. Effect of seed priming with AgNPs and CuNPs on α-amylase activity (μ mol/min/mg of protein) in greengram cv. DGGV-2 assessed at various post storage conditions under ambient environment.

Table 7
Synergistic effect of nanoprimed seeds that are stored for nine months and foliar application with AgNPs and CuNPs on plant height (cm) in greengram.

Treatments	30 DAS	60 DAS	At harvest
T$_1$: Primed seeds of AgNPs at 1000 ppm + Foliar application of AgNPs at 1000 ppm	35.96	46.48	53.00
T$_2$: Primed seeds of AgNPs at 1500 ppm + Foliar application of AgNPs at 1500 ppm	34.57	43.24	49.52
T$_3$: Primed seeds of AgNPs at 2000 ppm + Foliar application of AgNPs at 2000 ppm	32.17	38.55	43.21
T$_4$: Primed seeds of CuNPs at 1000 ppm + Foliar application of CuNPs at 1000 ppm	34.78	44.00	50.10
T$_5$: Primed seeds of CuNPs at 1500 ppm + Foliar application of CuNPs at 1500 ppm	31.87	37.76	42.94
T$_6$: Primed seeds of CuNPs at 2000 ppm + Foliar application of CuNPs at 2000 ppm	30.73	35.32	40.12
T$_7$: Castor (no foliar spay)	32.21	38.80	43.79
T$_8$: Deltamethrin (no foliar spray)	33.38	41.00	46.80
T$_9$: Control (untreated + no foliar spray)	30.56	34.67	39.00
S.Em ($\pm$)	0.27	0.53	0.65
C.D (1 %)	1.11	2.17	2.66
C.V.	1.44	2.31	2.49

3.3.2. Number of branches per plant

The data representing the effect of nanopriming and foliar application with silver and copper nanoparticles, synthesized using ocimum leaf extract, on the average number of branches in greengram plants at 30, 60 DAS (days after sowing), and harvest stages is observed in Table 8.

Significant differences in the number of branches were observed among the different treatments at all stages of the plant (30, 60 DAS, and at harvest). At the harvest stage, the number of branches remained consistent with the count observed at 60 DAS, regardless

Table 8
Synergistic effect of nanoprimed seeds that are stored for nine months and foliar application with AgNPs and CuNPs on number of branches plant^{-1} in greengram.

Treatments	30 DAS	60 DAS	At harvest
T_1: Primed seeds of AgNPs at 1000 ppm + Foliar application of AgNPs at 1000 ppm	4.65	5.61	5.61
T_2: Primed seeds of AgNPs at 1500 ppm + Foliar application of AgNPs at 1500 ppm	4.31	5.30	5.30
T_3: Primed seeds of AgNPs at 2000 ppm + Foliar application of AgNPs at 2000 ppm	3.63	4.60	4.60
T_4: Primed seeds of CuNPs at 1000 ppm + Foliar application of CuNPs at 1000 ppm	4.34	5.32	5.32
T_5: Primed seeds of CuNPs at 1500 ppm + Foliar application of CuNPs at 1500 ppm	3.60	4.58	4.58
T_6: Primed seeds of CuNPs at 2000 ppm + Foliar application of CuNPs at 2000 ppm	3.33	4.26	4.26
T_7: Castor (no foliar spay)	3.76	4.69	4.69
T_8: Deltamethrin (no foliar spray)	4.03	5.00	5.00
T_9: Control (untreated + no foliar spray)	3.27	4.20	4.20
S.Em ($\pm$)	0.05	0.07	0.07
C.D (1 %)	0.22	0.27	0.27
C.V.	2.39	2.35	2.35

of the treatment.

Seeds that underwent nanopriming and foliar spraying with AgNPs at a concentration of 1000 ppm exhibited the significantly higher number of branches, regardless of the plant age (30, 60 DAS, and at harvest) (T_1-4.65 plant^{-1}, 5.61 plant^{-1}, and 5.61 plant^{-1}, respectively), followed by seeds that were nanoprimed and foliar sprayed with CuNPs at 1000 ppm (T_4-4.34 plant^{-1}, 5.32 plant^{-1}, and 5.32 plant^{-1}, respectively). In contrast, the control had significantly fewer branches at 30, 60 DAS and at harvest (T_9-3.27 plant^{-1}, 4.20 plant^{-1}, and 4.20 plant^{-1} respectively) which were on par to the number of branches in seeds that were primed and foliar sprayed with CuNPs at 2000 ppm at 30, 60 DAS, and at harvest (T_6-3.33 plant^{-1}, 4.26 plant^{-1}, and 4.26 plant^{-1}, respectively).

3.3.3. Days to 50 % flowering

The average number of days taken for 50 % flowering in greengram plants, influenced by nanopriming and foliar application with silver and copper nanoparticles synthesized using ocimum leaf extract, is presented in Table 9.

There were no significant differences observed in the number of days taken for 50 % flowering between seeds that underwent priming and foliar application with AgNPs and CuNPs, seeds treated with castor oil and deltamethrin without foliar spray, and the control group. Numerically, the control group exhibited mean 50 % flowering on 40.33 days after sowing, while seeds that were primed and foliar sprayed with AgNPs at 1000 ppm showed mean 50 % flowering on 38.33 days after sowing. Here, days to 50 % flowering occurred two days earlier compared to the control group.

3.3.4. Number of pods per plant

Data recorded on the number of pods per plant in greengram affected by nanopriming and foliar application using silver and copper nanoparticles synthesized with ocimum leaf extract is presented in Table 9. The study found significant differences in the number of pods per plant among the different treatments.

The higher number of pods per plant was observed in plants derived from seeds that were primed and given foliar application with AgNPs at a concentration of 1000 ppm (T_1-13.83), which was statistically significant compared to other treatments. Followed by the seeds that were primed and foliar sprayed with CuNPs at 1000 ppm (T_4-12.70). In contrast, the control had significantly fewer pods per plant (T_9-9.00), which was on par with the number of pods per plant in seeds that were primed and foliar sprayed with CuNPs at 2000 ppm (T_6-9.11).

3.3.5. Seed yield per plant (g plant^{-1})

Table 9 provides data on the seed weight per plant in greengram influenced by nanopriming and foliar application with silver and copper nanoparticles synthesized using ocimum leaf extract. The study observed significant differences in seed weight per plant among the different treatments.

The higher seed yield per plant was recorded in plants derived from seeds that were nanoprimed and foliar sprayed with AgNPs at a concentration of 1000 ppm (T_1-3.75 g), which was statistically significant compared to other treatments. This was followed by the seeds that were primed and foliar sprayed with CuNPs at 1000 ppm (T_4-3.44 g). On the other hand, control seeds had significantly lower seed weight per plant (T_9-2.21 g), which was on par with the seed weight per plant in seeds that were primed and foliar sprayed with CuNPs at 2000 ppm (T_6-2.26 g).

3.3.6. Dehydrogenase activity (μg TPF g^{-1} soil day^{-1})

The data on the dehydrogenase activity in the soil of greengram crop, as influenced by nanopriming and foliar application with silver and copper nanoparticles synthesized using ocimum leaf extract, is mentioned in Fig. 17. The study observed non-significant variations in the dehydrogenase activity of soil among the different treatments.
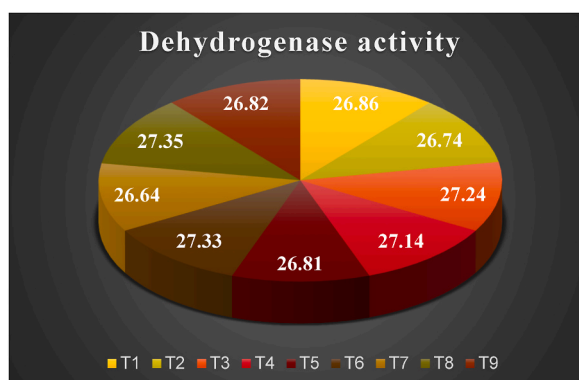
4. Discussion

Seeds play a critical role in agriculture as they serve as the primary source of new plant life. Seeds under storage are susceptible to

Table 9

Synergistic effect of nanoprimed seeds that are stored for nine months and foliar application with AgNPs and CuNPs on days to 50 % flowering, no. of pods plant^{-1} and seed yield per plant (g plant^{-1}) in greengram.

Treatments	50 % flowering	No. of pods plant^{-1}	Seed Yield (g plant^{-1})
T$_1$: Primed seeds of AgNPs at 1000 ppm + Foliar application of AgNPs at 1000 ppm	38.33	13.83	3.75
T$_2$: Primed seeds of AgNPs at 1500 ppm + Foliar application of AgNPs at 1500 ppm	38.67	12.63	3.39
T$_3$: Primed seeds of AgNPs at 2000 ppm + Foliar application of AgNPs at 2000 ppm	40.00	10.37	2.69
T$_4$: Primed seeds of CuNPs at 1000 ppm + Foliar application of CuNPs at 1000 ppm	38.67	12.70	3.44
T$_5$: Primed seeds of CuNPs at 1500 ppm + Foliar application of CuNPs at 1500 ppm	39.67	10.25	2.60
T$_6$: Primed seeds of CuNPs at 2000 ppm + Foliar application of CuNPs at 2000 ppm	40.00	9.11	2.26
T$_7$: Castor (no foliar spay)	39.67	10.42	2.78
T$_8$: Deltamethrin (no foliar spray)	39.67	11.52	3.10
T$_9$: Control (untreated + no foliar spray)	40.33	9.00	2.21
S.Em ($\pm$)	0.75	0.25	0.05
C.D (1 %)	NS	1.03	0.21
C.V.	3.31	3.94	3.13

Fig. 17. Synergistic effect of nanoprimed seeds that are stored for nine months and foliar application with AgNPs and CuNPs on dehydrogenase activity (μg TPF g^{-1} soil day^{-1}) in greengram.

pest infestations, leading to a detrimental impact on seed quality, vigour, and ultimately, crop productivity. While conventional insecticides and fumigants have been used to mitigate pest damage, their application often results in a rapid decline in seed germination rates. Furthermore, these chemical interventions pose environmental risks. As a result, there is a growing need for alternative and eco-friendly approaches to protect stored seeds from pests while preserving seed viability and reducing environmental harm. In recent decades, nanotechnology has emerged as a promising and versatile field, finding applications in diverse sectors, including agriculture. Among the cutting-edge applications, nanopriming has gained significant importance for enhancing seed performance and overall crop productivity.

4.1. Biosynthesis of silver and copper nanoparticles using ocimum leaf extract

Conventionally, nanomaterials were synthesized using chemical or physical methods [26]. However, these conventional techniques have been found to be capital-intensive and inefficient in terms of materials and energy usage [27]. In contrast, the biological method emerges as a promising substitute due to its non-toxic, cost-effective, and eco-friendly nature, eliminating the need for hazardous chemicals [28,29]. Biological synthesis involves nanoparticles' production without the use of reducing agents and stabilizers; instead, molecules produced by living organisms such as bacteria, fungi, yeast, algae, and plants act as natural nanofactories. Among the biological methods, green synthesis utilizing plant leaf extracts holds numerous advantages over chemical and physical approaches. Moreover, plant-mediated synthesis proves to be rapid, flexible, and well-suited for large-scale nanoparticle production [30]. The utilization of plant biodiversity has become widely recognized for synthesizing metal and metal oxide nanoparticles, owing to the abundance of effective phytochemicals found in various plant extracts, particularly leaves. These phytochemicals encompass a diverse range of compounds, including ketones, aldehydes, flavones, amides, terpenoids, carboxylic acids, phenols, and ascorbic acids [31]. Remarkably, these components possess the capacity to efficiently reduce metal salts, thereby facilitating the synthesis of metal nanoparticles. Consequently, for the present study, ocimum leaves were specifically chosen as the source for biosynthesizing silver and copper nanoparticles.

The reduction of Ag$^+$ to Ag^0 was visually monitored by observing the grey-black color, indicative of successful bio-reduction, consistent with previous studies [32,33]. The color of the AgNP colloid produced depends on the concentration of the added AgNO$_3$ solution [34]. The color change is attributed to the surface plasmon resonance of AgNPs in the visible region [35], and surface

active molecules present in the leaf extract, such as carbohydrates, flavonoids, and polyphenols, which also act as stabilizing agents during the synthesis [36,37]. Similarly, for CuNPs synthesis, the change in color from light green to dark green indicated the successful formation of copper nanoparticles, in line with previous studies [38–42]. The active molecules in the ocimum leaf extract acted as reducing and capping agents during the synthesis process. These standardized methods provide a reliable and environmentally friendly approach for the synthesis of AgNPs and CuNPs from ocimum leaf extract, offering a sustainable and efficient means for nanoparticle production.

4.2. Characterization of synthesized silver and copper nanoparticles

4.2.1. UV–Visible spectroscopy

The surface plasmon resonance (SPR) phenomenon arises when metallic nanoparticles (NPs) interact with light, leading to the coherent oscillation of conduction electrons in the metal. In the UV–Vis spectra recorded for the reaction solution of reduced silver nitrate using ocimum leaf extract, the silver nanoparticles exhibited a prominent absorption peak at 475 nm. This absorption maximum in the range of 400–500 nm is a characteristic feature of AgNPs due to their surface plasmon resonance [43,44]. Similar studies by Banerjee et al. [45], Krithiga et al. [46], and Pirtarighat et al. [47] also reported absorption maxima in the range of 425–475 nm for AgNPs synthesized using various plant leaf extracts. Overall, UV–Visible spectroscopy provided valuable insights into the successful synthesis of silver nanoparticles using ocimum leaf extract, and the observed SPR peak confirmed the presence of nanoparticles with specific optical properties.

In the case of copper nanoparticles biosynthesized through ocimum leaf extract, a strong SPR was observed at 322 nm due to the absorption of light by the NPs. These experimental findings are consistent with previous research by Fatma et al. [48] and Makvana et al. [49]. Joshi and Prakash [50] studied tulasi (*Ocimum tenuiflorum*) leaves and reported elevated peaks at 285 and 330 nm, while Shende et al. [51] achieved the biosynthesis of stable copper nanoparticles using *Ocimum sanctum* leaf extract, with UV–Vis spectroscopy showing absorption at 345 nm. It is noteworthy that the SPR of metallic compounds can vary with the size and shape of the nanoparticles [52,53]. Therefore, the specific SPR observed in the UV–Vis spectra of copper nanoparticles synthesized with ocimum leaf extract provides valuable insights into the size and properties of the nanoparticles, aiding in their characterization and understanding of their optical behavior.

4.2.2. Particle size analyzer (PSA)

The PSA instrument characterized the size distribution of AgNPs produced by ocimum leaf extract, with a mean diameter of 54.1 nm and 25 % of the distribution falling below 32.1 nm, confirming that the synthesized silver nanoparticles were in the nanoscale range. Lalitha et al. [54] reported a size range of 21.07 nm for the synthesized silver nanoparticles. Asmita et al. [55] conducted a study using neem leaves and found that the size of the silver nanoparticles was approximately 43 nm. The results obtained from PSA analysis by Iftikhar et al. [56] indicated a size range of 50–75 nm. Alqahtani et al. [57] also observed similar results, with a mean diameter of 52.8 nm reported by PSA.

For CuNPs, the mean diameter obtained from ocimum leaf extract was 74.9 nm, with 25 % of the distribution below 42.9 nm. Bai et al. [58] reported that the biosynthesized CuO NPs from *Moringa oleifera* exhibited a particle size range of 90 nm–250 nm, with over 50 % of frequencies falling between 130 nm and 170 nm. Kathad and Gajera [59] conducted a biological synthesis of copper nanoparticles from *Nag champa* and found the average particle size to be 135 nm. On the other hand, Iliger et al. [60] performed PSA analysis on CuNPs synthesized from Eucalyptus leaves and observed a size range of 60–75 nm, with an average size of 65 nm. The results from Zetasizer analysis by Usha et al. [41] revealed an average size of 37.61 nm for the biosynthesized copper nanoparticles.

Additionally, DLS provides valuable insights into the uniformity or heterogeneity of the particle size distribution, as described by the Polydispersity Index (PDI). The PDI offers a comprehensive view of the size distribution of scattered nanoparticles in the solution phase. An ideal nanoparticle PDI value is less than 0.5, indicating a relatively uniform size distribution. Conversely, higher PDI values suggest a more diverse range of particle sizes, leading to non-uniformity in the nanoparticle population [61]. In the case of silver and copper nanoparticles produced through bio-reduction using ocimum leaf extract, the polydispersity index values were found to be 0.419 and 0.466, respectively. These results indicate that the size distribution of the synthesized nanoparticles is relatively more homogeneous, as evidenced by the PDI values being less than 0.5. This uniformity in size distribution enhances the stability and performance of the nanoparticles.

4.2.3. Scanning electron microscope (SEM)

Characterization through SEM and EDX of silver nanoparticles biosynthesized through ocimum leaf extract revealed the shape of the nanoparticles to be round to spherical, and the EDX captured higher peaks that marked the presence of Ag as 83.58 per cent. The findings of this study are consistent with those of Rautela and Rani [62], who observed oval and spherical shapes for silver nanoparticles (AgNPs) using Field-Emission Scanning Electron Microscopy (FESEM). Elemental mapping of AgNPs by FESEM-EDX revealed the presence of 94 % silver and 6 % oxides, with a strong signal peak observed at 3 keV. Balkrishna et al. [63] also reported the formation of high-density, mostly spherical AgNPs in their study using SEM images, and EDX spectra showed strong signals for silver metal at 3 keV, along with other low-intensity peaks, possibly corresponding to carbon and oxygen, which could represent plant phytochemicals or biomass involved in stabilizing the AgNPs synthesized using the plant extract.

Characterization of copper nanoparticles synthesized through ocimum leaf extract using SEM and EDX revealed their spherical shape. Further analysis of the CuNPs through EDX profiling confirmed the presence of characteristic signals for copper and oxygen, with the chemical composition of copper being 81.36 %. These findings align with similar observations reported by Saranyaadevi et al.

[64], Hariprasad et al. [65], Usha et al. [41] and Kolahalam et al. [66], where copper nanoparticles were also found to be spherical in shape. Regarding the stabilization process of CuO nanoparticles, Sharma et al. [67] suggested that the peaks observed near 0 keV in the EDX spectra could be attributed to carbon and oxygen compounds present in the plant extract, which might be involved in stabilizing the CuO nanoparticles. Moreover, Saranyaadevi et al. [64], also reported that the copper nanoparticles exhibited absorption peaks of higher counts due to surface plasmon resonance in their study.

4.2.4. X-Ray diffraction (XRD)

The sharp and distinct peaks in AgNPs indicated the presence of face-centered cubic (fcc) symmetry and crystallinity. Similar diffraction patterns were reported by Hanna et al. [68], who synthesized silver nanoparticles from *Desertifilum tharense*, showing the same five main peaks corresponding to (101), (111), (200), (220), and (311) lattice planes.

The appearance of extra peaks in the XRD pattern can be attributed to the presence of phytochemical compounds in the leaf extracts used for nanoparticle synthesis. However, the stronger planes observed in the XRD pattern confirmed silver as a major constituent in the biosynthesis, consistent with findings by Kumar and Yadav [69] and Anandalakshmi et al. [70]. Bindhani and Panigrahi [71] also confirmed the presence of silver nanoparticles in the form of nanocrystals based on the peak positions at 2θ values of 38.28°, 44.04°, 64.34°, and 77.28° corresponding to (111), (200), (220), and (311) Bragg reflections, respectively, in accordance with the face-centered cubic structure of silver. These results align with previous studies conducted by Khan et al. [72], Tailor et al. [36], Melkamu et al. [73], and Balkrishna et al. [63], further supporting the crystalline nature and structural properties of the synthesized silver nanoparticles.

The high-angle peaks in the XRD analysis of CuNPs indicate the existence of a cubic-centered crystalline nature of the nanoparticles. These results are consistent with findings reported by Sumitha et al. [74], where major peak positions at 2θ values of 35.5° and 38.64° in the high-angle XRD of copper oxide nanoparticles synthesized from *Ocimum tenuiflorum* also confirmed the presence of a crystalline nature of the nanoparticles. The major peak positions closely matched the Joint Committee for Powdered X-ray Diffraction Standard (JCPDS no 02-1225). Similarly, Dagar et al. [42] reported the formation of copper nanoparticles with peaks in the range of 20°–40°, further confirming the crystalline nature of the nanoparticles. These findings are in line with other studies by Annapurna et al. [75], Amaliyah et al. [76], Nirmala et al. [30], and Ragunath et al. [77], which have consistently reported the crystalline nature of copper nanoparticles synthesized from various plant extracts.

4.2.5. Fourier transform infrared spectroscopy (FTIR)

FTIR spectrum of the silver nanoparticles displayed absorption peaks at specific wavenumbers. The peaks at 3849 cm^{-1}, 3745 cm^{-1}, and 3676 cm^{-1} are attributed to hydroxyl (OH) groups. This observation aligns with similar findings by Rani et al. [78]. The peaks at 3047 cm^{-1}, 2839 cm^{-1}, and 2619 cm^{-1} correspond to symmetric CH$_2$ stretching and C–H aldehydes groups, respectively [79]. The presence of nitrile and P–H ester stretching is indicated by the peak at 2337 cm^{-1} [80]. The peak at 2083 cm^{-1} corresponds to C–N stretching vibration [81]. The peak at 1882 cm^{-1} indicates an aromatic group, while the peaks at 1581 cm^{-1} and 1342 cm^{-1} are attributed to C≡N and C–N stretching of aromatic amine groups, respectively [63,82]. The peaks at 1226 cm^{-1} and 1022 cm^{-1} correspond to C–N stretching of amines and -C-O-C- stretching, respectively [45,83]. The peak at 802 cm^{-1} corresponds to aromatics, and the peak at 505 cm^{-1} indicates -C-I- stretching (alkyl halide) [84,85]. Overall, the FTIR spectrum exhibits distinctive peaks associated with hydroxyl, carbonyl, C≡C, amide, and amine groups, characteristic of polyphenols, alkaloids, flavonoids, fatty acids, amino acids, and enzymes/proteins [86], thereby indicating the presence of a capping agent with the nanoparticles.

The FTIR analysis of copper nanoparticles resulted in peaks at 1593 cm^{-1} is indicative of the presence of the C≡N functional group. Similarly, the peak at 459 cm^{-1} corresponds to the C–Cl functional group, as reported by Ghosh et al., [87]. The peak at 1519 cm^{-1} can be attributed to the N–H bond bending characteristic of an amine group, consistent with findings from Kolahalam et al. [66], and Kulkarni and Kulkarni [88]. The appearance of the peak at 1427 cm^{-1} is associated with the C–C stretching of an aromatic ring structure, as well as scissoring and bending vibrations of alkanes, as previously discussed by Shende et al., [51]. Peaks at 1361 cm^{-1} and 1354 cm^{-1} are related to the C–N stretching of amide functional groups. Additionally, the peak at 597 cm^{-1} corresponds to bending modes of vibrations involving the C–H bond, as noted in studies by Murthy et al., [89]. The presence of the peak at 1072 cm^{-1} signifies C–N stretching vibrations of aliphatic amines, with similar banding patterns observed at 852 cm^{-1} and 771 cm^{-1}, as documented in the copper nanoparticle synthesis study conducted by Melkamu et al., [73]. The peak at 771 cm^{-1} indicates C–H stretching, consistent with observations reported by Hariprasad et al., [65]. The FTIR spectrum of the copper nanoparticles suggests an interaction between functional groups within the plant extract and copper ions, leading to processes such as bio-reduction, formation, and stabilization of the synthesized copper nanoparticles.

Moreover, it is anticipated that the successful biofabrication of green-synthesized nanoparticles most likely occur through a donor-acceptor mechanism. This mechanism results from the interaction between the oxygen atoms of biofunctional groups (such as hydroxyl) present in tulasi leaf extract and the salt precursors (AgNO$_3$ and CuSO$_4$·5H$_2$O). The biosynthesis process for Tulasi leaf extract-mediated AgNPs and CuNPs could involve three phases: activation, growth, and termination. In the initial activation phase, Ag and Cu cations are extracted from silver nitrate and copper sulphate salt precursors, respectively, when dissolved in water. In the presence of biofunctional groups derived from tulasi, Ag and Cu cations undergo reduction to their metallic forms. Subsequently, during the growth and termination phases, the accumulation and stabilization of Ag and Cu nanoparticles are facilitated by the metabolites present in tulasi leaves. This results are in compliance with several reports indicating the biogenic synthesis of nanoparticles such as ZnO NPs [90] and Al$_2$O$_3$ NPs [91].

4.3. Influence of biosynthesized silver and copper nanoparticles against pulse beetles and on seed quality parameters of greengram during storage under lab conditions

In nanopriming, such as with AgNPs and CuNPs, a significant portion of nanomaterials adhere to the seed surface as coatings. This process allows for controlled water uptake and reduced gas permeability, contributing to more stable seed storage [92]. In the present study, greengram seeds were primed with AgNPs and CuNPs at various concentrations (1000, 1500, and 2000 ppm) and subjected to nine months of storage to assess their effects on seed quality and biochemical parameters, as well as seed infestation.

The results of the study revealed a gradual decline in seed quality attributes, including germination percentage, root length, shoot length, and vigour index during the entire storage period. This decline in seed quality can be attributed to the irreversible aging characteristics that affect living biological organisms, leading to deteriorative changes in the physical, physiological, and biochemical characteristics of seeds [20,93].

4.3.1. Germination percentage, root length, shoot length and seedling vigour index

The insecticidal properties of silver and copper nanoparticles proved effective in inhibiting pulse beetle multiplication, which significantly reduced seed damage and contributed to the enhanced germination rates compared to the control. Arumugam et al. [94] conducted a similar study and observed that silica nanotreated seeds at 1000 ppm of greengram showed complete retardation of pulse beetle growth. However, there was no negative effect on seed growth, as indicated by normal seed germination and the growth rate of root and shoot. Similarly, Wazid et al. [95] also conducted a study using copper nanoparticles, where seeds treated with copper nanoparticles at 1500 ppm demonstrated the higher seed germination rates, dehydrogenase enzyme activity, and the highest reduction in seed damage percentage compared to the control group. In the control group, the combination of seed damage and deterioration caused by insects led to more abnormal seedlings, resulting in decreased germination (39.67 %) by the end of the storage period. The current findings are also consistent with those of Parmar and Patel [96], who discovered mung bean susceptibility to *Callosobruchus chinensis* L. during storage. After six months of storage, *C. chinensis* exhibited a 29.97–65 per cent reduction in germination.

Even the germination rates of castor and deltamethrin treated seeds were found to be higher compared to the control group. However, the germination percentage of seeds treated with castor and deltamethrin was found to be significantly lower compared to seeds primed with AgNPs and CuNPs (1000 ppm) throughout the storage period. This observation indicates that nanoparticles play a vital role in enhancing the viability of seeds by offering protection. The enhanced germination can be attributed to the nanosized particles, allowing them to easily penetrate the seed coat and facilitate better absorption and utilization by the seeds [97]. Another study conducted on onion storage by Anandaraj and Natarajan [98] revealed that nanoparticles have a beneficial effect on improving seed quality. This effect may be attributed to nanoparticles inducing oxidation-reduction reactions *via* the superoxide ion radical during germination, resulting in the quenching of free radicals in germinating seeds. Moreover, Vashisth and Nagarajan [99] reported in maize that treating seeds with nanoparticles reversed the extent of deterioration caused by ageing, resulting in higher germination percentages.

From this study, it was also evident that higher concentrations of AgNPs (2000 ppm) and CuNPs (1500 ppm and 2000 ppm) resulted in lower germination rates compared to other treatments, except for the control. These findings align with the research conducted by Thuesombat et al. [100], who discovered that increased concentrations of AgNPs in jasmine rice led to reduced seed germination and subsequent seedling growth. The decreased germination observed at higher nanoparticle concentrations could be attributed to the increased absorption and accumulation of nanoparticles, both in the extracellular space and within the cells of the seeds. This accumulation may result in a reduction in cell division and cell elongation, as well as inhibition of the hydrolytic enzymes involved in food mobilization during the process of seed germination [101].

AgNPs and CuNPs (1000 ppm) consistently promoted the seedling growth characteristics of greengram throughout the storage period, outperforming the control. One main reason for this improvement is the decrease in seed infestation by insects, but the nanoparticles also demonstrated better performance compared to castor-treated and deltamethrin-treated seeds, even in cases where infestation was reduced. This enhancement in seedling length can be attributed to the activation of various metabolic pathways essential for seed germination, root and shoot growth, triggered by the nanoparticles accumulated within the seeds. Additionally, the effective mobilization of available food reserves in the seeds resulted in early emergence and growth of the seedlings, contributing to the increase in seedling growth [102]. In my findings, with an increase in concentrations of AgNPs and CuNPs, there was a decrease in seedling length. Previous studies have shown that the effect of AgNPs on seed germination and seedling growth can be positive or negative, depending on the size, properties, and concentration of the nanoparticles, the test plant, and the application method [103]. Another study reported a dose-dependent inhibitory effect of CuNPs on wheat root and shoot length has been evaluated, which supports the results of the current study. The reduction in root and shoot length may be due to changes in nitrate regulated auxin transport and cell death, resulting in the reduction of root development as well as shoot development [104].

4.3.2. Seed infestation percentage

Nanoparticles have been explored as a potential tool for integrated pest management (IPM) of stored grain pests, such as *C. maculatus*, as highlighted by Yang and Watts [105]. In the present study, all treatments exhibited a notable reduction in seed infestation percentage, throughout the nine-month storage period, except for the control group. Notably, seeds primed with AgNPs and CuNPs at concentrations of 1000, 1500, and 2000 ppm showed complete inhibition of insect multiplication, resulting in 100 % mortality of insects within the first month of storage. This impressive insecticidal effect can be attributed to the strong properties of AgNPs and CuNPs, which encompass insecticidal, bactericidal, antifungal, and antiviral activities [106,107], making them a promising candidate against insect pests. The absence of insect multiplication in nanoprimed seeds is likely due to the prevention of egg laying by

insects. A similar study by Arumugam et al. [94] also reported a drastic reduction in the fecundity of *C. maculatus* when exposed to silica nanoparticles, potentially due to desiccation and spiracular blockage. The reduced fecundity of insects could be attributed to the attachment of nanoparticles to the body of adult beetles, leading to suffering and the potential prevention of mating. Similar observations were made by Wazid et al. [95], who found that treatment with higher concentrations of biosynthesized CuNPs, specifically 1500 ppm and 1250 ppm, resulted in the highest adult mortality of 100 % and 0 % seed damage after 30 days of storage in chickpea seeds. Pavitra et al. [108] demonstrated that zinc oxide and copper nanoparticles, tested at various concentrations, exhibited a significant increase in mealybug mortality with a concentration of 2000 ppm.

On the contrary, the control group displayed a notable rise in the average count of both live and dead adult insects as the storage period advanced, primarily attributed to the rapid proliferation of insects. Consequently, this escalation in insect activity led to an amplified level of seed damage, intensifying as the storage duration increased. Similarly, seeds subjected to treatment with castor oil and deltamethrin also demonstrated effective control over seed damage, resulting in the absence of both live and deceased insects by the end of the initial month. This protective response persisted consistently throughout the entire nine-month storage duration, mirroring the behavior observed in seeds primed with nanoparticles. Nevertheless, despite this shared outcome in insect control, seeds primed with AgNPs and CuNPs (1000 ppm) displayed notable improvements in seed quality and biochemical parameters.

Only a limited number of studies have delved into the toxicokinetics or toxicodynamics of nanopesticides against storage grain insect pests, as these materials are relatively novel and remain subjects of ongoing exploration [109]. In my own study, noteworthy morphological variations were observed under a stereomicroscope in insects collected from seeds treated with AgNPs and CuNPs. Conversely, insects collected from the control seeds did not exhibit any such morphological variations (Fig. 15a and b). The observed morphological changes in insects found in seeds primed with nanoparticles included leg stretching, body twisting, and hind wing extension. These alterations could stem from sub-lethal effects incurred due to exposure to Ag and Cu nanoparticles. Sub-lethal effects encompass outcomes that may not result in immediate fatality but can profoundly influence the physiology, behavior, and development of the exposed organisms. Various factors might account for these morphological variations, such as neurotoxic impacts, disruption of growth and development, hormonal imbalances, oxidative stress, or disruptions in feeding behavior and reproductive success in pulse beetles.

Our study's findings parallel those of other research, wherein larvae of *Spodoptera litura* treated with nanoparticles displayed notable insecticidal activity and underwent significant developmental changes, as demonstrated by Vivekanandhan et al. [110]. Detailed scanning electron microscopic examinations of insects introduced to nanosilica-treated seeds clearly depicted nanoparticles adhering across the bodies of bruchid beetles, accompanied by scratches and splits on their cuticles. This phenomenon subsequently resulted in water loss due to dehydration, attributable to damage to the protective wax coating on the insect cuticle. Such damage could stem from both sorption and abrasion. This physical mode of action, hypothesized to underlie the observed effects, strengthens the viability of nanocides for storage pest management. Consequently, it is postulated that this mode of action of nanocides, primarily influencing behavior rather than genetic or physiological factors, could minimize the likelihood of genetic resistance or physiological adaptations, as elaborated by Arumugam et al. [94].

4.3.3. Biochemical parameters in seed

The excessive buildup of reactive oxygen species (ROS) leads to oxidative stress, posing a significant threat to seed viability during prolonged storage periods. Therefore, the presence of an efficient antioxidant system becomes essential to counteract the deleterious reactions that contribute to seed deterioration, as highlighted by Kaur et al. [111]. In the context of my investigation, an intriguing observation emerged during the initial month of storage: seeds that underwent priming with AgNPs and CuNPs (1000 ppm) exhibited the higher levels of catalase activity, and alpha-amylase content. As the storage duration progressed, a consistent downward trend was witnessed across all measured biochemical parameters, encompassing catalase activity and alpha-amylase concentration within greengram seeds. Remarkably, seeds subjected to priming with AgNPs and CuNPs (1000 ppm) exhibited a comparatively slower rate of decline in these pivotal biochemical indicators in contrast to all other treatments. Another investigation revealed a declining trend in catalase activity with prolonged storage, yet notably, seeds primed with TiO$_2$ @40 ppm exhibited the higher catalase activity [112]. Nano-primed seeds exhibit an elevated presence of antioxidant enzymes due to the stimulation induced by AgNPs-generated reactive oxygen species (ROS), which play a pivotal role in triggering seed germination [113]. Feizi et al. [114], reported the concept of oxidative windows, aligning with greater germination rates and accelerated seedling growth in nano-primed seeds when compared to both unprimed and traditionally primed seeds. The heightened α-amylase activity resulting from nano-priming treatment induces swift starch degradation during seed germination, indirectly contributing to an accelerated germination rate and enhanced seedling vigor [115].

Upon reaching the end of the nine-month storage period, a rapid decline in the biochemical parameters was notably observed in the control seeds. This phenomenon can be primarily attributed to enhanced insect infestation and the consequent seed damage, triggering the release of reactive oxygen species (ROS) and inducing oxidative stress. This heightened oxidative stress likely leads to an increased demand for catalase, aimed at mitigating the detrimental effects of ROS, consequently resulting in a reduction of catalase levels. Similar reductions in catalase activity due to insect feeding have been documented in various crop studies [116,117]. Insect infestation and the resulting damage can trigger stress responses within the seeds, diverting energy and resources away from normal metabolic processes. This diversion of resources may lead to decreased alpha amylase activity, affecting the breakdown of starch and consequently resulting in reduced levels of this enzyme. This decline in alpha amylase activity contributed to decreased germination in control seeds. The overall combination of reduced catalase activity and alpha amylase activity in control seeds accelerates their loss of vigor during storage, enhancing their susceptibility to rapid deterioration.

4.4. Influence of biosynthesized silver and copper nanoparticles on plant growth and seed yield of greengram under greenhouse conditions

Recognizing the benefits of foliar application involving nanoparticles, we conducted an experiment applying AgNPs and CuNPs through foliar means. In storage studies, it became evident that seeds primed with AgNPs and CuNPs at a concentration of 1000 ppm exhibited superior performance across all assessed parameters. However, within the controlled environment of the greenhouse, a distinct pattern emerged. Notably, plants derived from stored seeds that had undergone nanopriming with AgNPs at 1000 ppm and subsequently received foliar applications of AgNPs at the same concentration displayed the most noteworthy results. These plants demonstrated significant enhancements in critical growth and yield attributes, encompassing plant height, number of branches (at 30, 60, and harvest stages), as well as the number of pods and seed yield per plant. As foliar application concentrations increased, a parallel trend emerged akin to the findings observed with seed priming. Specifically, escalated concentrations of foliar application led to a decrease in plant growth and yield. Notably, the application of CuNPs at 2000 ppm to plants derived from stored seeds that had previously undergone nanopriming with CuNPs at 2000 ppm yielded results comparable to the control across all growth and yield parameters. This intriguing pattern underscores a key observation: when compared to AgNPs at higher concentrations, CuNPs at elevated levels demonstrate comparatively less plant growth and yield within the context of greengram plants. It was also observed that foliar application of AgNPs at 1000 ppm decreased the incidence of cercospora disease as well as leaf minor damage.

Supporting evidence for this experiment stems from previous research. For instance, Wang et al. [118] elucidated that AgNPs promote shoot length, root length, and plant height by stimulating cell division and elongation processes. Another contributing factor to the augmented growth observed with AgNPs could be the enhancement of chemical energy production in photosynthetic systems. The augmentation in photosynthetic pigments—comprising chlorophyll *a*, chlorophyll *b*, and carotenoids—has been identified as a catalyst for increased photosynthesis rates, culminating in heightened plant growth and weight. This mechanism was underscored by Govorov and Carmeli [119]. Further endorsement of the growth-enhancing effects of AgNPs can be found in Ansari et al. [120], findings, where the green synthesis of silver nanoparticles positively influenced tomato plant growth, development, productivity, and even resilience against pathogens when administered as a foliar spray. The enhancement in both yield and its components resulting from the foliar application of AgNPs can be attributed to several factors, including the amplification of growth parameters, photosynthetic pigments, and indole-3-acetic acid (IAA), as highlighted by Sadak, [121]. The escalation in plant growth attributed to varied concentrations of AgNPs is particularly tied to their influence on impeding ethylene signaling and augmenting electron exchange efficiency. This dual impact subsequently contributes to an overall increase in yield. This concept is echoed in the findings of Rezvani et al. [122] and Mehmood and Murtaza [123].

The outcomes of my investigation also revealed that the foliar application of AgNPs and CuNPs during the vegetative and foliar stages of greengram cultivation had no detrimental impact on soil microorganisms (Fig. 17). This evaluation was conducted by assessing the activity of the dehydrogenase enzyme with soil samples collected on the 45th day after sowing (DAS). The results indicated a non-significant variation compared to the control group, underscoring the absence of negative effects on soil microorganisms. These findings align with parallel studies. For instance, Arumugam et al. [94] reported that the application of silica nanoparticles to pulse seeds did not induce any discernible impact on soil microflora, as measured through colony forming units.

5. Conclusions

The properties of ocimum leaf extract, such as its reduction potential, capping and stabilizing abilities, and safety profile, make it a valuable and efficient natural agent in the green synthesis of silver and copper nanoparticles. The characterization process validated the synthesis, spherical morphology, presence of organic groups, and crystalline nature of both AgNPs and CuNPs. Additionally, the particle sizes fell comfortably within the Gaussian distribution, with an average size of 54.1 nm for AgNPs and 74.9 nm for CuNPs. The utilization of green-synthesized silver and copper nanoparticles (1000 ppm) through ocimum leaf extract offers a highly effective and environmentally friendly strategy for managing storage pests in pulses. AgNPs and CuNPs (1000 ppm) demonstrated strong anti-insecticidal (100 % mortality of bruchids) and antifungal properties, leading to substantial reductions in post-harvest losses and improved seed quality by enhancing catalase activity (0.682, 0.665 µ mol of H_2O_2 decomposed/min/mg of protein) and alpha amylase activity in storage. Silver nanoparticle foliar application at 1000 ppm not only ensured superior growth (35.96, 46.48 and 53.00 cm at 30, 60 DAS and at harvest respectively), yield (3.75 g plant^{-1}), and seed quality but also showed no adverse impact on soil microbial organisms, thus making them a promising and sustainable solution for the agricultural industry. In case of controlling the pulse beetles, both the nanoparticles have attributed to great antiinsecticidal nature. However, in improving seed quality throughout the storage period, AgNPs at 1000 ppm was found to be more effective. Also, when given foliar application of AgNPs at 1000 ppm to greengram plants grown from the stored seeds primed with AgNPs at 1000 ppm, superiority in terms of the growth, yield and quality were observed when compared to those with CuNPs.

Data availability

There is no extra data to be included in manuscript. All the data is available in the manuscript.

CRediT authorship contribution statement

M. Hemalatha: Writing – review & editing, Writing – original draft, Investigation, Formal analysis, Data curation. **J.S. Hilli:** Writing – review & editing, Resources, Funding acquisition, Conceptualization. **S.S. Chandrashekhar:** Writing – review & editing,

Supervision, Conceptualization. **A.G. Vijayakumar:** Writing – review & editing, Resources, Conceptualization. **Uday G. Reddy:** Writing – review & editing, Resources, Conceptualization. **P.S. Tippannavar:** Writing – review & editing, Conceptualization.

Declaration of competing interest

The authors declare that they have no known competing financial interests or personal relationships that could have appeared to influence the work reported in this paper.

References

[1] K. Neme, A. Nafady, S. Uddin, Y.B. Tola, Application of nanotechnology in agriculture, postharvest loss reduction and food processing: food security implication and challenges, Heliyon 7 (2021) e08539.
[2] C.B. Barrett, Overcoming global food security challenges through science and solidarity, Am. J. Agric. Econ. 103 (2021) 422–447.
[3] Anonymous, Communication from the commission to the European Parliament, the Council, the European Economic and Social Committee, and the Committee of the regions. A European Strategy for Key Enabling Technologies – A Bridge to Growth and Jobs, 2012, pp. 1–18.
[4] M. Sepahvand, F. Buazar, M.H. Sayahi, Novel marine-based gold nanocatalyst in solvent-free synthesis of polyhydroquinoline derivatives: green and sustainable protocol, Appl. Organomet. Chem. 34 (2020) e6000.
[5] S. Sundarrajan, R. Murugan, A.S. Nair, S. Ramakrishna, Fabrication of P3HT/PCBM solar cloth by electrospinning technique, Mater. Lett. 64 (2010) 2369–2372.
[6] U.K. Parashar, P.S. Saxena, A. Srivastava, Bioinspired synthesis of silver nanoparticles, Dig, J. Nanomater. Biostruct. 4 (2009) 159–166.
[7] H. Ma, M.M. Zangeneh, A. Zangeneh, H. Veisi, S. Hemmati, M. Pirhayati, B. Karmakar, Green decorated gold nanoparticles on magnetic nanoparticles mediated by Calendula extract for the study of preventive effects in streptozotocin-induced gestational diabetes mellitus rats, Inorg. Chem. Commun. 151 (2023) 110633.
[8] Anonymous, Introduction to Detia, Fumigation Detia export GmH, 2019, p. 3.
[9] Anonymous, Ministry of agriculture and farmers welfare, GOI, 2021-2022.
[10] M.G. Chaudhary, J.K. Malav, Y.B. Vala, N.A. Desai, Influences of different organic sources and seaweed extract on quality, nutrient content, uptake, soil fertility status and soil microbial population after harvest of summer greengram (*Vigna radiata* L.), J. Pharm. Innov. 10 (2021) 1390–1394.
[11] N. Yewle, K.C. Swain, S. Mann, P.N. Guru, Performance of hermetic bags in green gram [*Vigna radiata* (L.) R. Wilczek] storage for managing pulse beetle (*Callosobruchus chinensis*), J. Stored Prod. Res. 95 (2022) 101896.
[12] B. Poornasundari, D. Thilagavathy, Pest control in green gram seeds (*Vigna radiata*) by using plant extracts, Int. Lett. Nat. Sci. 40 (2015).
[13] G.B. Hosamani, R.R. Patil, S.S. Chandrashekhar, V.I. Benagi, B.S. Nandihalli, Sunlight mediated green synthesis of silver nanoparticles from soybean seed and its bio-efficacy on *Callosobruchus chinensis* (L.), J. Exp. Zool. 23 (2020) 1091–1095.
[14] M.N. Nadagouda, G. Hoag, J. Collins, R.S. Varma, Green synthesis of Au nanostructures at room temperature using biodegradable plant surfactants, Cryst. Growth Des. 9 (2009) 4979–4983.
[15] M.T. El-Saadony, M.E. Abd El-Hack, A.E. Taha, M.M. Fouda, J.S.N. Ajarem, S. Maodaa, N. Elshaer, Ecofriendly synthesis and insecticidal application of copper nanoparticles against the storage pest *Tribolium castaneum*, J. Nanomater. 10 (2020) 587.
[16] D. Gautam, K.G. Dolma, B. Khandelwal, M. Gupta, M. Singh, T. Mahboob, V. Nissapatorn, Green synthesis of silver nanoparticles using *Ocimum sanctum* Linn. and its antibacterial activity against multidrug resistant *Acinetobacter baumannii*, PeerJ 11 (2023) e15590.
[17] J.M. Dhotare, M.G. Rathod, P.D. Barkhude, G.T. Kamble, N.V. Dongrajkar, S.N. Shivankar, A.P. Pathak, Green synthesis of copper nanoparticles by using aqueous extract of *Ocimum sanctum* leaves and its antibacterial activity, World J. Biol. Pharm. Health Sci. 13 (2023) 15–23.
[18] A. Annapoorna, K.A. Jaleeli, T. Sreekanth, A. Ahmad, Synthesis of Ag, Cu and Ag-Cu bimetallic nanoparticles using tulasi leaf extract, Int. J. Adv. Sci. Technol. 29 (2020) 1353–1360.
[19] ISTA Anonymous, International Seed Testing Association), International rules for seed testing, Seed Sci. Technol. 27 (2011) 25–30.
[20] A.A. Abdul-Baki, J.D. Anderson, Vigour determination in soybean seeds by multiple criteria, Crop Sci. 13 (1973) 630–633.
[21] C.B. Sibakwe, T. Donga, Laboratory assessment of the levels of resistance in some bean varieties infested with bean weevils (*Acanthoscelides obtectus* and *Zabrotes subfasciatus*), Int. j. plant soil sci. 4 (2015) 124–131.
[22] S. Sadasivam, A. Manikam, Biochemical Methods for Agricultural Sciences, Wiley Eastern Limited, New Delhi, India, 1992, pp. 184–185.
[23] R.F. Beers, L.W. Sizer, A spectrophotometric method for measuring the breakdown of hydrogen peroxide by catalase, J. Biol. Chem. 195 (1952) 133–140.
[24] R. David Lide, Handbook of Chemistry and Physics, CRC Press, Boca Raton, Florida, 1998, pp. 3–318.
[25] L. Casida, D. Klein, T. Santoro, Soil dehydrogenase activity, Soil Sci. 98 (1964) 371–376.
[26] A. Leela, M. Vivekanandan, Tapping the unexploited plant resources for the synthesis of silver nanoparticles, Afr. J. Biotechnol. 7 (2008).
[27] C. Ramteke, T. Chakrabarti, B.K. Sarangi, R.A. Pandey, Synthesis of silver nanoparticles from the aqueous extract of leaves of *Ocimum sanctum* for enhanced antibacterial activity, J. Chem. (2013) 1–7.
[28] P. Mohanpuria, N. Rana, S. Yadav, Biosynthesis of nanoparticles: technological concepts and future applications, J. Nanoparticle Res. 10 (2008) 507–517.
[29] C.L. Keat, A. Aziz, A.M. Eid, N.A. Elmarzugi, Biosynthesis of nanoparticles and silver nanoparticles, Bioresour. Bioprocess. 2 (2015) 1–11.
[30] M. Nirmala, B. Kavitha, S. Nasreen, S. Kiruthika, B. Divya, E. Manochitra, Green synthesis of copper nanoparticles using *Ocimum sanctum* L. (Tulasi) and *Piper nigrum* L. (Pepper seed) for pollution free environment, World Sci. News 150 (2020) 105–117.
[31] J. Singh, T. Dutta, K.H. Kim, M. Rawat, P. Samddar, P. Kumar, Greensynthesis of metals and their oxide nanoparticles: applications for environmental remediation, J. Nanobiotechnol. 16 (2018) 1–24.
[32] D. Philip, *Mangifera indica* leaf-assisted biosynthesis of well-dispersed silver nanoparticles, Spectrochim. Acta Mol. Biomol. Spectrosc. 78 (2011) 327–331.
[33] A.M. Awwad, N.M. Salem, Green synthesis of silver nanoparticles by mulberry leaves extract, J. Nanosci. Nanotechnol. 2 (2012) 125–128.
[34] H.I. Badiah, F. Seedeh, G. Supriyanto, A.H. Zaidan, Synthesis of silver nanoparticles and the development in analysis method, in: IOP Conference Series: Earth and Environmental Science, IOP Publishing, 2019 012005 vol. 217.
[35] P. Mukherjee, M. Roy, B.P. Mandal, G.K. Dey, P.K. Mukherjee, J. Ghatak, A.K. Tyagi, S.P. Kale, Green synthesis of highly stabilized nanocrystalline silver particles by a non-pathogenic and agriculturally important fungus T. *asperellum*, Nanotechnology 19 (2008) 075103.
[36] G. Tailor, B.L. Yadav, J. Chaudhary, M. Joshi, C. Suvalka, Green synthesis of silver nanoparticles using *Ocimum canum* and their anti-bacterial activity, Biochem. Biophys. Rep. 24 (2020) 100848.
[37] N. Liaqat, N. Jahan, T. Anwar, H. Qureshi, Green synthesized silver nanoparticles: optimization, characterization, antimicrobial activity and cytotoxicity study by hemolysis assay, Front. Chem. 10 (2022) 952006.
[38] S. Thakur, R.S. Rai, S. Sharma, Study the antibacterial activity of copper nanoparticles synthesized using herbal plants leaf extracts, Int. J. Biotechnol. 4 (2014) 21–34.
[39] J. Mekala, M.R. Rajan, R. Ramesh, Green synthesis and characterization of copper nanoparticles using tulasi (*Ocimum sanctum*) leaf extract, Indian J. Sci. Res. 5 (2016) 14–16.
[40] M. Altikatoglu, A. Attar, F. Erci, C.M. Cristache, I. Isildak, Green synthesis of copper oxide nanoparticles using *Ocimum basilicum* extract and their antibacterial activity, Fresenius Environ. Bull. 25 (2017) 7832–7837.

[41] S. Usha, K.T. Ramappa, S. Hiregoudar, G.D. Vasanthkumar, D.S. Aswathanarayana, Biosynthesis and characterization of copper nanoparticles from tulasi (*Ocimum sanctum* L.) leaves, Int. j. curr. microbiol. appl. sci. 6 (2017) 2219–2228.

[42] K.S. Dagar, I. Shah, K. Kumari, K. Pal, G.B. Narula, K. Soni, Green synthesis of copper nanoparticles designed from *Ocimum sanctum* for purification of waste water, J. Therm. Anal. Calorim. 1 (2020) 32–40.

[43] J.M. Ashraf, M.A. Ansari, H.M. Khan, M.A. Alzohairy, I. Choi, Green synthesis of silver nanoparticles and characterization of their inhibitory effects on AGEs formation using biophysical techniques, Sci. Rep. 6 (2016) 20414.

[44] E.S. Al-Sheddi, N.N. Farshori, M.M. Al-Oqail, S.M. Al-Massaran, Q. Saquib, R. Wahab, J. Musarrat, A.A. Al-Khedhairy, M.A. Siddiqui, Anticancer potential of green synthesized silver nanoparticles using extract of *Nepeta deflersiana* against human cervical cancer cells (HeLA), Bioinorgan. Chem. Appl. 21 (2018) 1–12.

[45] P. Banerjee, M. Satapathy, A. Mukhopahayay, P. Das, Leaf extract mediated green synthesis of silver nanoparticles from widely available Indian plants: synthesis, characterization, antimicrobial property and toxicity analysis, Bioresour. Bioprocess. 1 (2014) 1–10.

[46] N. Krithiga, A. Rajalakshmi, A. Jayachitra, Green synthesis of silver nanoparticles using leaf extracts of *Clitoria ternatea* and *Solanum nigrum* and study of its antibacterial effect against common nosocomial pathogens, j. nanosci. (2015) 1–8.

[47] S. Pirtarighat, M. Ghannadnia, S. Baghshahi, Green synthesis of silver nanoparticles using the plant extract of *Salvia spinosa* grown in vitro and their antibacterial activity assessment, J. nanostructure chem. 9 (2019) 1–9.

[48] S. Fatma, P. Kalainila, E. Ravindran, S. Renganathan, Green synthesis of copper nanoparticle from *Passiflora foetida* leaf extract and its antibacterial activity, Asian J. Pharmaceut. Clin. Res. (2017) 79–83.

[49] C. Makvana, Faruk Arodiya, Kokila Parmar, Green synthesis of polymer-capped copper nanoparticles using *Ocimum sanctum* leaf extract: antibacterial and antioxidant potential, Biosci. Biotechnol. Res. Commun. 14 (2021) 1832–1838.

[50] N.C. Joshi, Prakash, Leaves extract-based biogenic synthesis of cupric oxide nanoparticles, characterizations, and antimicrobial activity, Asian J. Pharmaceut. Clin. Res. 12 (2019) 288–291.

[51] S. Shende, N. Gaikwad, S. Bansod, Synthesis and evaluation of antimicrobial potential of copper nanoparticle against agriculturally important phytopathogens, Synth. Met. 1 (2016) 41–47.

[52] G. Oberdorster, E. Oberdorster, J. Oberdorster, Nanotoxicology: an emerging discipline evolving from studies of ultrafine particles, Environ. Health Perspect. 113 (2005) 823–839.

[53] E.M. Soylu, S. Soylu, S. Kurt, Antimicrobial activities of the essential oils of various plants against tomato late blight disease agent Phytophthora infestans, Mycopathologia 161 (2006) 119–128.

[54] A. Lalitha, R. Subbaiya, P. Ponmurugan, Green synthesis of silver nanoparticles from leaf extract *Azhadirachta indica* and to study its anti-bacterial and antioxidant property, Int. j. curr. microbiol. appl. sci. 2 (2013) 228–235.

[55] J.G. Asmita, P. Padmanabhan, P.K. Suresh, N.J. Suresh, Synthesis of silver nanoparticles using extract of neem leaf and triphala and evaluation of their antimicrobial activities, Int. J. Pharma Bio Sci. (2012) 6279–6299.

[56] M. Iftikhar, M. Zahoor, S. Naz, N. Nazir, G.E.S. Batiha, R. Ullah, H.M. Mahmood, Green synthesis of silver nanoparticles using *Grewia optiva* leaf aqueous extract and isolated compounds as reducing agent and their biological activities, J. Nanomater. (2020) 1–10.

[57] Y.S. Alqahtani, A. Bahafi, K.K. Mirajkar, R.R. Basavaraju, S. Mitra, S.S. More, I.A. Shaikh, In vitro antibacterial activity of green synthesized silver nanoparticles using *Mangifera indica* aqueous leaf extract against multidrug-resistant pathogens, J. Antibiot. 11 (2022) 1503.

[58] B. Bai, S. Saranya, V. Dheepaasri, S. Muniasamy, N.S. Alharbi, B. Selvaraj, B.M. Gnanamangai, Biosynthesized copper oxide nanoparticles (CuO NPs) enhances the anti-biofilm efficacy against *K. pneumoniae* and *S. aureus*, J. King Saud Univ. Sci. 34 (2022) 102120.

[59] U. Kathad, H.P. Gajera, Synthesis of copper nanoparticles by two different methods and size comparison, Int. J. Pharma Bio Sci. 5 (2014) 533–540.

[60] K.S. Iliger, T.A. Sofi, N.A. Bhat, F.A. Ahanger, J.C. Sekhar, A.Z. Elhendi, F. Khan, Copper nanoparticles: green synthesis and managing fruit rot disease of chilli caused by *Colletotrichum capsici*, Saudi J. Biol. Sci. 28 (2021) 1477–1486.

[61] A.K. Roddu, A.W. Wahab, A. Ahmad, P. Taba, Green-route synthesis and characterization of the silver nanoparticles resulted by bio-reduction process, J. Phys. Conf. 1341 (3) (2019) 032004. IOP Publishing.

[62] A. Rautela, J. Rani, Green synthesis of silver nanoparticles from *Tectona grandis* seeds extract: characterization and mechanism of antimicrobial action on different microorganisms, J. Anal. Sci. Technol. 10 (2019) 1–10.

[63] A. Balkrishna, N. Thakur, B. Patial, S. Sharma, A. Kumar, V. Arya, R. Amarowicz, Synthesis, characterization and antibacterial efficacy of *Catharanthus roseus* and *Ocimum tenuiflorum*-mediated silver nanoparticles: phytonanotechnology in disease management, Processes 11 (2023) 1479.

[64] K. Saranyaadevi, V. Subha, R.E. Ravindran, S. Renganathan, Synthesis and characterization of copper nanoparticle using *Capparis zeylanica* leaf extract, Int. J. ChemTech Res. 6 (2014) 4533–4541.

[65] S. Hariprasad, G.S. Bai, J. Santhoshkumar, C.H. Madhu, D. Sravan, Green synthesis of copper nanoparticles by *Areva lanata* leaves extract and their antimicrobial activities, Int. J. ChemTech Res. 9 (2016) 98–105.

[66] L.A. Kolahalam, K.R.S. Prasad, P.M. Krishna, N. Supraja, S. Shanmugan, The exploration of bio-inspired copper oxide nanoparticles: synthesis, characterization and in-vitro biological investigations, Heliyon 8 (2022) e09726.

[67] S. Sharma, K. Kumar, N. Thakur, S. Chauhan, M.S. Chauhan, Eco-friendly *Ocimum tenuiflorum* green route synthesis of CuO nanoparticles: characterizations on photocatalytic and antibacterial activities, J. Environ. Chem. Eng. 9 (2021) 105395.

[68] A.L. Hanna, H.M. Hamouda, H.A. Goda, M.W. Sadik, F.S. Moghanm, A.M. Ghoneim, T.R. Elsayed, Biosynthesis and characterization of silver nanoparticles produced by *Phormidium ambiguum* and *Desertifilum tharense* cyanobacteria, Bioinorgan. Chem. Appl. 22 (2022) 1–14.

[69] V. Kumar, S.K. Yadav, Plant mediated synthesis of silver and gold nanoparticles and their applications, J. Chem. Technol. Biotechnol. 84 (2009) 151–157.

[70] K. Anandalakshmi, J. Venugobal, V.J. Ramasamy, Characterization of silver nanoparticles by green synthesis method using *Pedalium murex* leaf extract and their antibacterial activity, Appl. Nanosci. 6 (2016) 399–408.

[71] B.K. Bindhani, A.K. Panigrahi, Biosynthesis and characterization of silver nanoparticles (SNPs) by using leaf extracts of *Ocimum Sanctum* L. (Tulasi) and study of its antibacterial activities, J. Nanomed. Nanotechnol. 6 (2015) 2157–7439.

[72] M.Z.H. Khan, F.K. Tarek, M. Nuzat, M.A. Momin, M.R. Hasan, Rapid biological synthesis of silver nanoparticles from *Ocimum sanctum* and their characterization, j. nanosci. 17 (2017) 1–7.

[73] Z. Melkamu, P.R. Jeyaramraja, T. Paulos, Optimization of the synthesis of silver nanoparticles using the leaf extract of Ocimum sanctum and evaluation of their antioxidant potential, Nano express 3 (2022) 035006.

[74] S. Sumitha, R. Vidhya, M.S. Lakshmi, K.S. Prasad, Leaf extract mediated green synthesis of copper oxide nanoparticles using *Ocimum tenuiflorum* and its characterization, Int. J. Chem. Sci. 14 (2016) 435–440.

[75] S. Annapurna, Y. Suresh, B. Sreedhar, G. Bhikshamaiah, A. Singh, Characterization of green synthesized copper nanoparticles stabilized by ocimum leaf extract, Mater. Res. Soc. Symp. Proc. 17 (2014) 2–8.

[76] S. Amaliyah, D.P. Pangesti, M. Masruri, A. Sabarudin, S.B. Sumitro, Green synthesis and characterization of copper nanoparticles using *Piper retrofractum* Vahl extract as bioreductor and capping agent, Heliyon 6 (2020) e04636.

[77] L. RagunathSuresh, M. Sankaran, R.S. Kumar, A.I. Almansour, N. Arumugam, Synthesis and characterization of copper oxide nanoparticles using rambutan peel extract via greener route, Rasayan J. Chem. 14 (2021) 2660–2665.

[78] S.S. Rani, C.G.L. Justin, K. Gunasekaran, S.S.J. Roseleen, Efficacy of green synthesized silver nanoparticle, plant powders and oil against rice weevil *Sitophilus oryzae* L. (Coleoptera: *Curculionidae*) on sorghum seeds, J. Pharmacogn. Phytochem. 8 (2019) 38–42.

[79] F. Zia, N. Ghafoor, M. Iqbal, S. Mehboob, Green synthesis and characterization of silver nanoparticles using *Cydonia oblong* seed extract, Appl. Nanosci. 6 (2016) 1023–1029.

[80] M.A. Ahmad, S. Salmiati, M. Marpongahtun, M.R. Salim, J.A. Lolo, A. Syafiuddin, Green synthesis of silver nanoparticles using *Muntingia calabura* leaf extract and evaluation of antibacterial activities, Biointerface Res. Appl. Chem. 10 (2020) 6253–6261.

[81] P. Devaraj, C. Aarti, P. Kumari, Synthesis and characterization of silver nanoparticles using *Tabernae montana* divaricata and its cytotoxic activity against MCF7 cell line, Int. J. Pharm. Pharmaceut. Sci. 6 (2014) 86–90.

[82] G. Anuradha, S.B. Sundar, M.V. Raman, J.S. Kumar, T. Sujath, Single step synthesis and characterization of silver nanoparticles from *Ocimum tenuiflorum* L. green and purple, IOSR J. Appl. Chem. 7 (2014) 123–127.

[83] K. Jyoti, M. Baunthiyal, A. Singh, Characterization of silver nanoparticles synthesized using *Urtica dioica* Linn. leaves and their synergistic effects with antibiotics, J. Radiat. Res. Appl. Sci. 9 (2016) 217–227.

[84] N. Siddharthan, G. Kalaivani, E. Poongothai, M. Arul, N. Hemalatha, Characterization of silver nanoparticles synthesized from *catheranthus roseus* (*vinca rosea*) plant leaf extract and their antibacterial activity, Int. J. Res. Anal. Rev. 6 (2019) 680–685.

[85] O.A. Ojo, B.E. Oyinloye, A.B. Ojo, B.O. Ajiboye, I.I. Olayide, O. Idowu, F. Adewunmi, Green-route mediated synthesis of silver nanoparticles (AgNPs) from *Syzygium cumini* (L.) Skeels polyphenolic-rich leaf extracts and investigation of their antimicrobial activity, IET Nanobiotechnol. 12 (2018) 305–310.

[86] C. Krishnaraj, R. Ramachandran, K. Mohan, P.T. Kalaichelvan, Optimization for rapid synthesis of silver nanoparticles and its effect on phytopathogenic fungi, Spectrochim. Acta: Mol. Biomol. Spectrosc. 93 (2012) 95–99.

[87] M.K. Ghosh, S. Sahu, I. Gupta, T.K. Ghorai, Green synthesis of copper nanoparticles from an extract of *Jatropha curcas* leaves: characterization, optical properties, CT-DNA binding and photocatalytic activity, RSC Adv. 10 (2020) 22027–22035.

[88] V.D. Kulkarni, P.S. Kulkarni, Green synthesis of copper nanoparticles using *Ocimum Sanctum* leaf extract, Int. J. Chem. Stud. 1 (2013) 2321–4902.

[89] H.C. Murthy, T. Desalegn, M. Kassa, B. Abebe, T. Assefa, Synthesis of green copper nanoparticles using medicinal plant *Hagenia abyssinica* (Brace) JF. Gmel. leaf extract: antimicrobial properties, J. Nanomater. (2020) 1–12.

[90] T. Khalafi, F. Buazar, K. Ghanemi, Phycosynthesis and enhanced photocatalytic activity of zinc oxide nanoparticles toward organosulfur pollutants, Sci. Rep. 9 (2019) 6866.

[91] H. Koopi, F. Buazar, A novel one-pot biosynthesis of pure alpha aluminum oxide nanoparticles using the macroalgae Sargassum ilicifolium: a green marine approach, Ceram. Int. 44 (2018) 8940–8945.

[92] A. Shelar, A.V. Singh, R.S. Maharjan, P. Laux, A. Luch, D. Gemmati, R. Patil, Sustainable agriculture through multidisciplinary seed nanopriming: prospects of opportunities and challenges, Cells 10 (2021) 2428.

[93] E.H. Roberts, in: E.H. Roberts (Ed.), Cytological, Genetical and Metabolic Changes in Seed Viability Associated with Loss of Viability of Seeds, Chapman and Hall Ltd, London, 1972, pp. 253–306.

[94] G. Arumugam, V. Velayutham, S. Shanmugavel, J. Sundaram, Efficacy of nanostructured silica as a stored pulse protector against the infestation of bruchid beetle, *Callosobruchus maculatus* (Coleoptera: Bruchidae), Appl. Nanosci. 6 (2016) 445–450.

[95] Sushila Nadagouda Wazid, A. Prabhuraj, R. Harishchanra Naik, N.M. Shakuntala, H. Sharanagouda, Effect of biosynthesized copper green nanoparticles on pulse beetle, *Callosobruchus analis* (Coleoptera: *Chrysomelidae*), Int. J. Chem. Stud. 7 (2019) 2217–2221.

[96] R.V. Parmar, B.H. Patel, Susceptibility of mung bean varieties to *Callosobruchus chinensis* under storage conditions, Legume Res. 39 (2016) 637–642.

[97] Dangi Sandeep, N.K. Biradarpatil, V.K. Deshpande, Ravi Hunje, Suma Mogali, Effect of seed treatment with nanoparticles on seed storability of Soybean, Int. j. curr. microbiol. appl. sci. 8 (2019) 2535–2545.

[98] K. Anandaraj, N. Natarajan, Effect of nanoparticles for seed quality enhancement in Onion [*Allium cepa* (Linn) cv. CO (On)] 5, Int. j. curr. microbiol. appl. sci. 6 (2017) 3714–3724.

[99] A. Vashisth, S. Nagarajan, Germination characteristics of seeds of maize (*Zea mays* L.) exposed to magnetic fields under accelerated ageing condition, J. Agric. Phys. 9 (2009) 50–58.

[100] P. Thuesombat, S. Hannongbua, S. Akasit, S. Chadchawan, Effect of silver nanoparticles on rice (*Oryza sativa* L. cv. KDML 105) seed germination and seedling growth, Ecotoxicol. Environ. Saf. 104 (2014) 302–309.

[101] P. Korishettar, S.N. Vasudevan, N.M. Shakuntala, S.R. Doddagoudar, S. Hiregoudar, B. Kisan, Seed polymer coating with Zn and Fe nanoparticles: an innovative seed quality enhancement technique in pigeonpea, J. Appl. Nat. Sci. 8 (2016) 445–450.

[102] S.J. Lakshmi, R.R. Bai, H. Sharanagouda, C.T. Ramachandra, S. Nadagouda, S.R. Doddagoudar, Biosynthesis and characterization of ZnO nanoparticles from spinach (*Spinacia oleracea*) leaves and its effect on seed quality parameters of greengram (*Vigna radiata*), Int. J. Curr. Microbiol. Appl. Sci. 6 (2017) 3376–3384.

[103] A.A. Feregrino-Perez, E. Magaña-López, C. Guzmán, K. Esquivel, A general overview of the benefits and possible negative effects of the nanotechnology in horticulture, Sci. Hortic. 238 (2020) 126–137.

[104] N. Thakur, S. Chrungoo, S. Rana, S. Kaur, S. Kaur, A. Pathak, Effect of copper nanoparticles on in-vitro seed germination of wheat *(Triticum Aestivum L.)* Varieties, Int. J. Pharmaceut. Sci. Res. 12 (2021) 4307–4313.

[105] L. Yang, D.J. Watts, Particle surface characteristics may play an important role in Phytotoxicity of alumina nanoparticles, Toxicol. Lett. 158 (2005) 122–132.

[106] M. Rai, K. Kon, A. Ingle, N. Duran, S. Galdiero, M. Galdiero, Broad-spectrum bioactivities of silver nanoparticles: the emerging trends and future prospects, Appl. Microbiol. Biotechnol. 98 (2014) 1951–1961.

[107] G.D. Saratale, R.G. Saratale, G. Benelli, G. Kumar, A. Pugazhendhi, D.S. Kim, H.S. Shin, Anti-diabetic potential of silver nanoparticles synthesized with *Argyreia nervosa* leaf extract high synergistic antibacterial activity with standard antibiotics against foodborne bacteria, J. Cluster Sci. 28 (2017) 1709–1727.

[108] G. Pavitra, N. Sushila, A.G. Sreenivas, J. Ashoka, H. Sharanagouda, Effect of green zinc and copper nanoparticles on Cotton mealybug, *Phenacoccus solenopsis* Tinsley, Int. J. Curr. Microbiol. Appl. Sci. 11 (2020) 899–907.

[109] P. Jasrotia, M. Nagpal, C.N. Mishra, A.K. Sharma, S. Kumar, U. Kamble, G.P. Singh, Nanomaterials for postharvest management of insect pests: current state and future perspectives, Front. Nanotechnol. 3 (2022).

[110] P. Vivekanandhan, S. Bedini, M.S. Shivakumar, Isolation and identification of entomopathogenic fungus from Eastern Ghats of South Indian forest soil and their efficacy as biopesticide for mosquito control, Parasitol. Int. 76 (2021) 102099.

[111] R. Kaur, J. Chandra, S. Keshavkant, Nanotechnology: an efficient approach for rejuvenation of aged seeds, Physiol. Mol. Biol. Plants 27 (2021) 399–415.

[112] S. Khan, A. Dayal, N. Thomas, P.K. Shukla, Effect of titanium dioxide (TiO$_2$) nanoparticles on the storability of onion (*Allium cepa* L.) seeds under ambient condition, Environ. Conserv. 24 (2023) 1–15.

[113] U. Chandrasekaran, X. Luo, Q. Wang, K. Shu, Are there unidentified factors involved in the germination of nano-primed seeds? Front. Plant Sci. 11 (2020) 832.

[114] H. Feizi, P.R. Moghaddam, N. Shahtahmassebi, A. Fotovat, Assessment of concentrations of nano and bulk iron oxide particles on early growth of wheat (*Triticum aestivum* L.), Annu. Res. Rev. Biol. (2013) 752–761.

[115] W. Mahakham, A.K. Sarmah, S. Maensiri, P. Theerakulpisut, Nano-priming technology for enhancing germination and starch metabolism of aged rice seeds using phyto-synthesized silver nanoparticles, Sci. Rep. 7 (2017) 8263.

[116] H. Khattab, The defense mechanism of cabbage plant against phloem-sucking aphid (Brevicoryne brassicae L.), Aust. j. basic appl. sci. 1 (2007) 56–62.

[117] G.K. Taggar, R.S. Gill, A.K. Gupta, J.S. Sandhu, Fluctuations in peroxidase and catalase activities of resistant and susceptible black gram (*Vigna mungo* (L.) Hepper) genotypes elicited by *Bemisia tabaci* (Gennadius) feeding, Plant Signal. Behav. 7 (2012) 1321–1329.

[118] W. Wang, Y. Ren, J. He, L. Zhang, X. Wang, Z. Cui, Impact of copper oxide nanoparticles on the germination, seedling growth, and physiological responses in *Brassica pekinensis* L, Environ. Sci. Pollut. Res. 27 (2020) 31505–31515.

[119] A.O. Govorov, I. Carmeli, Hybrid structures composed of photosynthetic system and metal nanoparticles: plasmon enhancement effect, Nano Lett. 7 (2007) 620–625.

[120] M. Ansari, S. Ahmed, A. Abbasi, N.A. Hamad, H.M. Ali, M.T. Khan, Q.U. Zaman, Green synthesized silver nanoparticles: a novel approach for the enhanced growth and yield of Tomato against early blight disease, Microorganisms 11 (2023) 886.

[121] M.S. Sadak, Impact of silver nanoparticles on plant growth, some biochemical aspects and yield of fenugreek plant (*Trigonella foenum-graecum*), Bull. Natl. Res. Cent. 43 (2019) 1–6.

[122] N. Rezvani, A. Sorooshzadeh, N. Farhadi, Effect of nano-silver on growth of saffron in flooding stress, World Acad, Eng. Technol. 1 (2012) 517–522.

[123] A. Mehmood, G. Murtaza, Application of SNPs to improve yield of *Pisum sativum* L. (pea), IET Nanobiotechnol. 11 (2017) 390–394.